ORIGINAL ARTICLE

Heterocyclic chalcone (E)-1-(2-hydroxy-3,4,6-trimethoxyphenyl)-3-(thiophen-2-yl) prop-2-en-1-one derived from a natural product with antinociceptive, anti-inflammatory, and hypoglycemic effect in adult zebrafish

Maria Kueirislene Amancio Ferreira[1] · Wendy Pascoal Oliveira Freitas[1] · Italo Moura Barbosa[1] ·
Matheus Nunes da Rocha[1] · Antônio Wlisses da Silva[2] · Emanuela de Lima Rebouças[2] ·
Francisco Rogênio da Silva Mendes[3] · Carlucio Roberto Alves[4] · Paulo Iury Gomes Nunes[7] ·
Márcia Machado Marinho[5] · Roselayne Ferro Furtado[6] · Flávia Almeida Santos[7] · Emmanuel Silva Marinho[1] ·
Jane Eire Silva Alencar de Menezes[1] · Helcio Silva dos Santos[1,2,5]

Abstract

Diabetes is a disease linked to pathologies, such as chronic inflammation, neuropathy, and pain. The synthesis by the Claisen–Schmidt condensation reaction aims to obtain medium to high yield chalconic derivatives. Studies for the synthesis of new chalcone molecules aim at the structural manipulation of aromatic rings, as well as the replacement of rings by heterocycles, and combination through chemical reactions of synthesized structures with other molecules, in order to enhance biological activity. A chalcone was synthesized and evaluated for its antinociceptive, anti-inflammatory and hypoglycemic effect in adult zebrafish. In addition to reducing nociceptive behavior, chalcone (40 mg/kg) reversed post-treatment-induced acute and chronic hyperglycemia and reduced carrageenan-induced abdominal edema in zebrafish. It also showed an inhibitory effect on NO production in J774A.1 cells. When compared with the control groups, the oxidative stress generated after chronic hyperglycemia and after induction of abdominal edema was significantly reduced by chalcone. Molecular docking simulations of chalcone with Cox -1, Cox-2, and TRPA1 channel enzymes were performed and indicated that chalcone has a higher affinity for the COX-1 enzyme and 4 interactions with the TRPA1 channel. Chalcone also showed good pharmacokinetic properties as assessed by ADMET.

Keywords Chalcone · Zebrafish · Molecular docking · Natural product

✉ Helcio Silva dos Santos
helciodossantos@gmail.com

1 Laboratório de Química de Produtos Naturais-LQPNS, Universidade Estadual do Ceará, Programa de Pós-Graduação em Ciências Naturais, Fortaleza, CE, Brazil

2 Programa de Doutorado em Biotecnologia, Rede Nordeste de Biotecnologia (RENORBIO), Fortaleza, CE, Brazil

3 Programa de Pós-Graduação em Química Biologica, Universidade Regional do Cariri, Crato, CE, Brasil

4 Laboratório de Sistemas de Nanotecnologia e BiomateriaisPrograma de Pós-Graduação em Ciências Naturais, Universidade Estadual do Ceará, Fortaleza, CE, Brazil

5 Departamento de Química, Universidade Estadual Vale do Acaraú, Sobral, CE, Brazil

6 Embrapa Agroindústria Tropical, Fortaleza, CE, Brazil

7 Departamento de Fisiologia e Farmacologia Laboratório de Produtos Naturais, Faculdade de Medicina, Universidade Federal do Ceará, Fortaleza, CE, Brazil

Introduction

Diabetes mellitus (DM) is a severe chronic metabolic disorder, categorized into two types: DM-I, which is generated by pancreatic β-cell dysfunction, while DM-II is caused by impaired insulin secretion due to resistance to insulin and disturbances in glucose homeostasis occur (Rammohan et al. 2020). In this sense, DM-II, associated with insulin resistance and obesity in adults, is approximately nine times more common than DM-I, commonly diagnosed in children (Ranjan and Sharma 2020). This disease affects approximately 100 million people, and treatments for it are considered inadequate, mainly due to the lack of understanding of the pathophysiological mechanisms of the disease. Diabetes can even lead to organ or tissue damage due to multiple complications, including an increase in the level of reactive oxygen species (ROS) (Asmat et al. 2016). Notably, the disease is also linked to pathologies such as chronic inflammation, neuropathy, and pain (Grosick et al. 2017).

In light of this, several recent studies have advanced understanding of the role of TRP channels in pain and type 2 diabetes (DM2), particularly how TRP-targeted drugs may become valuable alternatives to current pharmaceutical treatments for these diseases. TRP channels are a family of cation channels involved in various cellular and sensory signaling pathways. In mice and zebrafish, formalin, for example, is a chemical that can deactivate TRPA1 (McNamara et al. 2007; Silva et al. 2020; Jaqueline et al. 2021) and promotes a biphasic nociception response, which it divides into neurogenic and inflammatory responses as a result of tissue reactions caused by inflammation (Barr 1998).
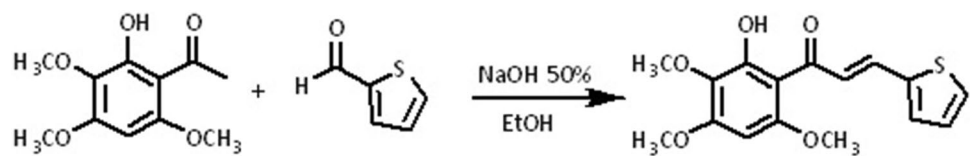
Administration of carrageenan (Cg) is commonly used to cause inflammation in rodents. Several animal studies have shown that exposure to Cg causes inflammation, which is characterized by increased vascular permeability, which leads to extravasation of plasma fluids and migration of leukocytes to the inflamed area (Winter et al. 1962; Cunha et al. 2016). Inflammation is widely recognized as an important etiologic factor that plays a vital role in developing insulin resistance, significantly contributing to DM2. In addition, it aids in the prevention of diabetes complications. This hypothesis was proposed based on the findings of several studies that focused on the link between the development of type 2 diabetes, an increase in circulatory levels of inflammatory markers in the acute phase, and insulin resistance (Halim and Halim 2019). In this way, inflammatory responses may establish a causal relationship with the onset of DM2, which further contributes to insulin resistance, or they may increase due to a hyperglycemic state, which leads to the complications of DM2 (Cruz et al. 2013).

Despite the medications currently approved and used for the treatment of type 2 diabetes, the scientific community is working to develop more effective, safe, and affordable natural and/or synthetic antidiabetic agents that can overcome the side effects of current medications, such as metformin (a drug commonly used to treat type 2 diabetes) which causes gastrointestinal disturbances, such as diarrhea, nausea, and abdominal discomfort, and Vitamin B12 deficiency in some patients (Arslanian et al. 2013). Chalcones have shown promising antidiabetic activity through the modulation of various molecular targets (Adelusi et al. 2021). Owing to the number and positions of various substituents, including hydroxy, methoxy, methyl, prenyl, geranyl, lavandulyl, pyran, furan, and glycosyl derivatives, chalcones have a central scaffold of 1,3-diaryl-2-propen-1-one with great structural diversity (Ferreira et al. 2021). The chalcone synthesized in this study is a heterocyclic chalcone, and these are considered promising because they have heterocyclic rings, as well as in the drugs developed, such as captopril and diazepam (DZP), and when observing the chemical structure of the drugs used in therapies, approximately 62% of them are heterocyclic (Qadir et al. 2022).

Zebrafish is a model that has been widely used to understand the pathophysiological mechanisms of the inflammatory process (Belo et al. 2021; Rebouças et al. 2021), Diabetes (Lakstygal et al. 2019; Coutinho et al. 2022), pain (Silva et al. 2020; Jaqueline et al. 2021) and other pathologies. Nearly all human DM-related genes have zebrafish orthologs, with an average genetic homology of nearly 70% across species (Lakstygal et al. 2019). Furthermore, the ease of exposure to the drug by immersion in water Gleeson et al. (2007) allows inducing MD-like states in zebrafish by housing the fish in a solution of glucose (Rammohan et al. 2020) and sucrose (Rebouças et al. 2021).

Regarding the fish nociception model, the nociceptive physiology is well established and similar to that of mammals (Sneddon 2002; Esancy et al. 2018). Zebrafish have receptors for histamine (Peitsaro et al. 2000), opioids (Gonzalez-Nunez et al. 2013), transient receptor potential cation channels (TRPs; TRPV1 e TRPA1) (Gau et al. 2013). Thus, zebrafish have the necessary cellular components to respond to various noxious stimuli. The present study evaluated a new synthetic chalcone for its antinociceptive, anti-inflammatory, and hypoglycemic effect in adult zebrafish. In addition, in silico studies were conducted with specific molecular targets of diabetes, inflammation and pain to assess possible structural interactions of chalcone with these targets.

Scheme 1 Synthesis of chalcone

Materials and methods

Drugs and reagents

Formaldehyde, acetic acid (Dynamics, Brazil); Dimethyl sulfoxide (DMSO; Dynamic®); Morphine (Cristalia). 2′,7′-dihydrodichlorofluorescein diacetate (DCHF-DA, Sigma-Aldrich).

Synthesis and chemical characterization of chalcone

A description of the procedure for the synthesis of chalcone is shown in Scheme 1. (*E*)-1-(2-hydroxy-3,4,6-trimethoxyphenyl)-3-(thiophen-2-yl) prop-2-en-1-one was synthesized using a Claisen–Schmidt condensation reaction in a basic medium. First, an ethanol solution of 2-hydroxy-3,4,6-trimethoxyacetophenone isolated from *Croton anisodontus* (2 mmol) was added to a solution of thiophene-2-carbaldehyde (2 mmol), followed by the addition of 10 drops of 50% w/v aqueous NaOH and stirred for 48 h at 32 °C (Scheme 1). Chalcone was then filtered under reduced pressure, washed with cold water, dried, and recrystallized from ethanol. The structure of the heterocyclic chalcone was confirmed by analyzing the ^{1}H, ^{13}C and infrared spectra (Figs. S1–S4, Supplementary material), which were obtained using a Bruker DPX-300 Platform operating at frequencies of 300 MHz for hydrogen and 75 MHz for carbon. The infrared absorption spectrum was obtained using a Bruker vacuum spectrometer (VERTEX 70 V). A chromatographic evaluation was performed by HPLC (Agilent 1260 Infinity, Germany).

Biological evaluation

Toxicity in adult Zebrafish (ZFa)

The test was based on the (Arellano-Aguiar et al. 2015) methodology with adaptations. The Zfa (*n = 6* group) were treated with the intraperitoneal chalcone (i.p.; 20 μL) at doses (4, 20, and 40 mg/kg.). Dimethyl sulfoxide (DMSO 3%; 20 μL, i.p.) was used as a negative control. After 24, 48, 72, and 96 h, the number of animals killed was counted, and the data were subjected to statistical analysis using the Trimmed Spearman−Karber method with 95% confidence intervals, where the lethal dose to kill 50% was estimated (LD_{50}) of animals.

Locomotor activity

Animals (*n = 6*/group) were pretreated (20 μL; *i.p.*) with the chalcone in the same doses analyzed in Sect. 2.3.1. Diazepam (Dzp; 40 mg/kg) or vehicle (DMSO 3%) were used as positive and negative controls, respectively. After 30 min of the treatments, the animals were added individually to glass Petri dishes (10 × 15 cm; with quadrants at the bottom of the plate) containing the same water from the aquarium (Magalhães et al. 2017). A group without treatments (Naive) was included. The number of line crossings was recorded during 0 to 5 min.

Behavioral antinociceptive activity

Nociceptive agents (5 mL; i.m (intramuscular)) and antagonists (20 mL; i.p) were used, as well as the time of analysis of the nociceptive behavior (Batista et al. 2018; Silva et al. 2020), formalin (0 0.1%; transient receptor potential of subfamily A member 1 cation channel [TRPA1], an agonist) and camphor (30.4 mg/kg; TRPA1 antagonist). After treatment with chalcone, 30 min before nociceptive application, the animals were placed in a glass Petri dish (10 × 15 cm), and the response to the nociceptive behavior was observed in the neurogenic phase (0–5 min) and the inflammatory phase (15–30 min). The animals' behavior was recorded and analyzed by experimenters unaware of the treatment.

Formalin-induced nociceptive behavior

Adult zebrafish (*n = 6*/) were pretreated (20 μL; i.p) with the synthesized chalcone (4, 20 or 40 mg/kg), morphine (8 mg/kg; positive control) and vehicle (negative control).; 3% DMSO), 30 min before the intramuscular injection of formalin applied to the animals' tail. A naive group (*n = 6*; untreated) were also included. The number of crosses in the open field was counted both in the neurogenic phase (0–5 min) and in the inflammatory phase (15–30 min) (Silva et al. 2020). Em seguida, os animais foram pré-tratados intraperitonealmente com a cânfora antagonista (30,4 mg/kg; 20 μL; ip), 15 min antes da chalcona (40 mg/kg; 20 μL; i.p), para verificar possível envolvimento de o sistema TRPA1.

In vitro *In vitro toxicity on PC12 cells*: To explore the potential of this compound as a therapeutic agent for the

treatment of diseases related to the nervous system, such as diabetic neuropathy, chronic pain, and neurodegenerative inflammatory conditions, we used the PC12 cell line, as it has been used as a model in several studies in the evaluation of neurotoxicity (Yang et al. 2017; Wiatrak et al. 2020). For in vitro assays, the stock solution (0.2 M) of the chalcone was prepared with sterile DMSO, and working solutions were diluted with sterile PBS to guarantee a maximum of 0.5% DMSO concentration in experimental groups.

Cytotoxicity of chalcone in PC12 cells was assessed by MTT assay, as described elsewhere (Mosmann 1983a). Briefly, 10^5 cells/mL were plated in 96-well plates with 10% FBS DMEM (Dulbecco's Modified Eagle Medium) overnight at 37 °C and 5% CO_2 atmosphere. After, cells were treated with Cth (1000–15.6 μM) for 24 h. Then, experimental groups were incubated with MTT (2.5 mg/mL) for 4 h, and DMSO was added to dissolve the formazan salt. The absorbance was measured at 570 nm. DMSO 0.5% and PBS were used as the negative control.

Cell culture: The murine macrophage lineage J774A.1, obtained from the Rio de Janeiro Cell Bank (BCRJ), was used for cell culture. Cells were cultured in DMEM (Dulbecco's Modified Eagle's Medium) supplemented with 10% fetal bovine serum (FBS), containing 100 U/mL of penicillin and 100 μg/mL of streptomycin, in a humidified atmosphere at 37 °C and 5% of CO_2.

Sample dilution and sample number: The samples were previously solubilized in supplemented DMEM containing 1% DMSO (vehicle), following the necessary dilutions to obtain the concentrations recommended in each test. All assays were performed in experimental triplicate ($n = 6$).

Cell viability assay by the MTT method: Cell viability was assessed using the MTT (3-[4,5-dimethylthiazol-2-yl]-2,5-diphenyl tetrazolium) assay. (Mosmann 1983b). J744A.1 cells were seeded at a density of $1 \times 10\ 5$ cells/well, in a 96-well plate and incubated for 24 h. Cells were treated with chalcone (0.24–250 μM) for 24 h. MTT (1 mg/mL) was added to each cell well and incubated for 4 h at 37 °C. Then, the medium was removed, and DMSO (150 μL) was added to each well. After 30 min of incubation, the absorbance was measured at 570 nm using a microplate reader (Asys UVM 340, Biochrom, USA). The percentage of cell viability inhibition was calculated compared to the vehicle group (100% viability).

Evaluation of the inhibition of nitric oxide (NO) production stimulated by LPS: The concentration of nitrate/nitrite in the medium was measured as an indicator of NO production according to the Griess reaction. J744A.1 cells were seeded at a density of 5×105 cells/well, in a 96-well plate and treated with chalcone at different concentrations (0.24–3.91 μM) for 1 h and then stimulated with LPS (1 μg/mL) at 37 °C for 24 h. Dexamethasone (40 μM) was used as a positive control. For analysis, the culture supernatant was

collected and mixed with an equal volume of Griess reagent (1% sulfanilamide, 0.1% N-[1-naphthyl]-ethylenediamine dihydrochloride, 5% phosphoric acid), and the absorbance measured at 540 nm, using a microplate reader (Asys UVM 340, Biochrom, USA). The amount of nitrate/nitrite in the samples was calculated from a standard curve of sodium nitrite (De Brito et al. 2021).

Statistical analysis: The results were expressed as mean $\pm$ standard deviation of mean (S.D.). All data were evaluated under their normal distribution using the Kolmogorov–Smirnov test. One-way ANOVA was used for multiple comparisons of parameters, with the level of significance between the groups determined by Tukey's post test. Values of $p < 0.05$ were considered statistically significant. All data were analyzed using GraphPad Prism® 5.03 software (San Diego, Califórnia, EUA).

In vivo *Toxicity in adult Zebrafish (ZFa)*: The test was based on the (Arellano-Aguiar et al. 2015) methodology with adaptations. The Zfa ($n = 6$ group) were treated with the intraperitoneal chalcone (*i.p.*; 20 μL) at doses (4, 20, and 40 mg/kg.). Dimethyl sulfoxide (DMSO 3%; 20 μL, i.p.) was used as a negative control. After 24, 48, 72, and 96 h, the number of animals killed was counted, and the data subjected to statistical analysis using the Trimmed Spearman−Karber method with 95% confidence intervals, where the lethal dose to kill 50% was estimated (LD_{50}) of animals.

Locomotor activity: Animals ($n = 6$/group) were pretreated (20 μL; *i.p.*) with the chalcone in the same doses analyzed in Sect. 2.3.1. Diazepam (Dzp; 40 mg/kg) or vehicle (DMSO 3%) were used as positive and negative controls, respectively. After 30 min of the treatments, the animals were added individually to glass Petri dishes (10×15 cm; with quadrants at the bottom of the plate) containing the same water from the aquarium (Magalhães et al. 2017). A group without treatments (Naive) was included. The number of line crossings was recorded during 0 to 5 min.

Behavioral antinociceptive activity: Nociceptive agents (5 mL; i.m (intramuscular)) and antagonists (20 mL; i.p) were used, as well as the time of analysis of the nociceptive behavior (Batista et al. 2018; Silva et al. 2020), formalin (0.1%; transient receptor potential of subfamily A member 1 cation channel [TRPA1], an agonist) and camphor (30.4 mg/kg; TRPA1 antagonist). After treatment with chalcone, 30 min before nociceptive application, the animals were placed in a glass Petri dish (10×15 cm), and the response to the nociceptive behavior was observed in the neurogenic phase (0–5 min) and the inflammatory phase (15–30 min). The animals' behavior was recorded and analyzed by experimenters unaware of the treatment.

Formalin-induced nociceptive behavior: Adult zebrafish ($n = 6$/) were pretreated (20 μL; i.p) with the synthesized chalcone (4, 20 or 40 mg/kg), morphine (8 mg/

kg; positive control) and vehicle (negative control).; 3% DMSO), 30 min before the intramuscular injection of formalin applied to the animals' tail. A naive group ($n = 6$; untreated) were also included. The number of crosses in the open field was counted both in the neurogenic phase (0–5 min) and in the inflammatory phase (15–30 min) (Silva et al. 2020). Em seguida, os animais foram pré-tratados intraperitonealmente com a cânfora antagonista (30,4 mg/kg; 20 μL; ip), 15 min antes da chalcona (40 mg/kg; 20 μL; i.p), para verificar possível envolvimento de o sistema TRPA1.

Anti-inflammatory activity: Abdominal edema was induced by carrageenan in adult zebrafish (Batista et al. 2018). Adult animals ($n = 6$) received chalcone (40 mg/kg; 20 μL; i.p.) vehicle (Control, 3% DMSO; 20 μL; i.p.) or ibuprofen (positive control, 100 mg/kg; 20 μL i.p.), after 1 h before the treatments received injection of 1.5% carrageenan (20 μL; i.p.). The animals were weighed before the treatments and 4 h after the carrageenan application. The fish were sacrificed in an ice bath (4ºC) after the experiment, and the liver tissues were removed for analysis of oxidative stress (Sect. 2.3.6.5.1).

Levels of reactive oxygen species (ROS): The assay used 2′,7′ dihydrodichlorofluorescein diacetate (DCHF-DA). Liver tissues from three animals (in duplicate) were macerated in Tris−HCl−EDTA followed by centrifugation (10,000 g × 10 min). 50 μl of the supernatant was collected and mixed with 5 μl of DCHF-DA. The oxidation of DCHF-DA to fluorescent dichlorofluorescein was measured to detect ROS. The emission of fluorescence intensity from DCF was recorded at 520 nm (with excitation of 480 nm) 2 h after adding DCHF-DA to the sample. Protein concentration was determined using the UV−VIS light spectrophotometry method at 280 nm and a standard curve of bovine serum albumin (BSA) (Loetchutinat et al. 2005).

Hypoglycemic effect of chalcone *Sucrose-induced acute hyperglycemia*: Acute hyperglycemia was established using 20 μL by intraperitoneal (i.p.) injection of sucrose (2.5 g/kg body weight) in adult zebrafish (CEUA-UECE; nº 04983945/2021). First, groups of animals ($n = 6$/group) were treated intraperitoneally with sucrose (2.5 mg/kg; 20 μL). Then, 30 min later, the hyperglycemic groups were treated with 3% DMSO (20 μL), insulin (1 IU; subcutaneous—SC), and metformin hydrochloride (200 mg/kg, 20 μL; i.p.). An untreated group was included (Naive). After 1 h and 30 min of treatments, the animals were euthanized by inducing hypothermia with water and ice at 0 and 3 °C. Blood glucose readings were taken by placing a glucometer test strip (Active, Accu Check) directly on the severed tail of each animal. The results were expressed as mean values ± standard error of the mean and submitted to analysis of variance (one-way ANOVA), followed by Tukey's test.

Sucrose-induced chronic hyperglycemia: The induction of hyperglycemia in adult zebrafish was performed based on the methodology of Ranjana and Sharma (2020) with modifications. Animals ($n = 6$ / group) were immersed in sucrose solution (83.25 mM/L) in dechlorinated water in 5 L glass aquaria for seven days. The sucrose solution was changed every day at the same time. On the 8th day, the animals were removed from the glucose solution and kept until the 11th day in dechlorinated water. (There were no animal deaths during the induction of hyperglycemia).

The groups of animals ($n = 6$/group) that spent the seven days submerged in sucrose were pretreated orally (using an automatic 20 μL pipette) after 12 h of fasting for four days (at the same time) with the chalcone (40 mg/kg; 20 μL). Other groups of animals ($n = 6$ / group) were treated with controls—Acarbose (300 mg/kg; 20 μL; positive control), Metformin (200 mg/kg; 20 μL; positive control), or 3% DMSO. (Drug Diluent; Negative Control). A group of untreated zebrafish was included (Naive).

Blood glucose levels were measured on the fourth day after 4 h of treatments. Before blood collection, the animals were euthanized (by inducing hypothermia with water and ice at 0 and 3 °C), then blood glucose readings were taken by placing a glucometer test strip (Active, Accu Check) directly on each animal's severed tail (Coutinho et al. 2022).

Reactive oxygen species (ROS) levels in the liver and brain of hyperglycemic Zebrafish: Oxidative stress was evaluated in the treated animals during the four days (described above). Groups of animals ($n = 6$/group) sacrificed for glycemic testing had their liver and brain removed. The assay used 2', 7' dihydrodichlorofluorescein diacetate (DCHF-DA). Liver and brain tissues from two animals (in triplicate) were macerated in Tris−HCl−EDTA followed by centrifugation (10,000 g × 10 min). The supernatant was collected (50 μl) and mixed with 5 μl of DCHF-DA. The oxidation of DCHF-DA to fluorescent dichlorofluorescein was measured to detect ROS. The emission of fluorescence intensity from DCF was recorded at 520 nm (with excitation of 480 nm) 2 h after adding DCHF-DA to the sample. Protein concentration was determined using the UV light spectrophotometry method at 280 nm using a standard curve of bovine serum albumin (BSA) (Loetchutinat et al. 2005).

Statistical analysis: The results were expressed as mean values ± standard error of mean for each group of 6 animals. After confirming the normality of distribution and homogeneity of the data, the differences between the groups were submitted to analysis of variance (one-way ANOVA), followed by Tukey's test. All analyzes were performed using GraphPad Prism v. 8.0. The level of statistical significance was set at 5% ($p < 0.05$).

Molecular docking

To carry out the simulations, the codes used were:Autodocktools ™, AutoDockVina ™ (Trott and Olson 2010b), Avogadro ™ (http://avogadro.cc/) (Hanwell et al. 2012), Discovery studio visualizer ™ viewer (Biovia 2016), Gabedit 2.5.0 (Allouche 2011), Gaussian 09 software (Frisch et al. 2016), Marvin ™ 19.8, 2020, (http://www.chemaxon.com), Pymol (DeLano 2020) and UCSF Chimera ™.

Ligand preparation and optimization

The Chalcone molecule was geometrically optimized using the Density Functional Theory (DFT) method at the B3LYP/6–311 + + G(d,p) computational level (Ditchfield et al. 1971; Lee et al. 1988; Becke 1992) in the gas phase using the Gaussian 09 software (Frisch et al. 2016). From the optimized geometry, the molecular electrostatic potential was computed at the same level of theory, and the isosurface was rendered (isovalue = 0.01) with the Gabedit 2.5.0 software (Allouche 2011).

General docking procedures

To carry out the molecular docking studies of hypoglycemic activity, the enzyme *maltase-glucoamylase C-terminal subunit* (CtMGAM) was selected as a target. CtMGAM is involved in the production of glucose in the human lumen, being considered an excellent target for the study of drug development for type 2 diabetes (Ren et al. 2011). To obtain the three-dimensional coordinates of the CtMGAM, the data available in the Protein Data Bank-RCSB repository was used (https://www.rcsb.org/). The structure of CtMGAM (PDB-codex 3TOP) was resolved by X-ray diffraction, and the crystal was obtained with a resolution of 2.88 Å, classified as a hydrolase/hydrolase inhibitor from the *Homo sapiens* organism, being expressed in the *Komagataella pastoris* system (Ren et al. 2011). CtMGAM was co-crystallized with the α-acarbose inhibitor (PRD_900007) which was subjected to a re-docking procedure.

For the studies of the anti-inflammatory activity, the enzymes Cyclooxygenase-1 (COX-1) that is deposited in the Protein Data Bank—RCSB (https://www.rcsb.org/) with the title "Crystal Structure of Cyclooxygenase-1 in Complex with Flurbiprofen", with code 3N8Z, being classified as a nonmutant oxidoreductase from the organism *ovis aries* expressed in the *Spodoptera frugiperda* system. The structure of COX-1 was resolved by X-ray diffraction, with a Resolution of 2.90 Å(Sidhu et al. 2010). Another enzyme used in the molecular docking study of the anti-inflammatory potential was Cyclooxygenase-1 (COX-1) which is deposited in the Protein Data Bank—RCSB (https://www.rcsb.org/) under the title "The Structure of Vioxx Bound to Human COX-2", with code 5KIR, being classified as a nonmutant oxidoreductase from the organism *Homo sapiens* expressed in the *Spodoptera frugiperda* system. The structure of COX-2 was resolved by X-ray diffraction, with a Resolution of 2.70 Å(Orlando and Malkowski 2016).

For studies of antinociceptive activity, the structure of the transient potential receptor of ankyrin 1-TRPA1 was chosen, which was obtained from the Protein Data Bank (https://www.rcsb.org/), identified as "Structure of human TRPA1 in complex with agonist GNE551" (PDB 6X2J). The structure was deposited in the Protein Data Bank with a resolution of 3.00 Å, being determined by electron microscopy, classified as membrane protein/agonist, *Homo sapiens* organism, *Spodoptera frugiperda* expression system (Liu et al. 2021).

To carry out the molecular docking simulations, the code was chosen. AutoDock Vina (Trott and Olson 2010a), is configured to run the Lamarckian Genetic Algorithm–LGA. The grid boxes were centered to encompass all protein chains to determine the simulation space. For CtMGAM, the grid box was centered at coordinates − 45,828, 21,487, and 17,927 for the *x*, *y*, and *z* axes respectively with size parameters 126 Å(*x*), 82 Å(*y*) and 124 Å(*z*).

For COX-1 enzymes, the grid box was centered at coordinates − 30,781, 56,507, and − 11,092 for the *x*, *y*, and *z* axes, respectively, with size parameters 114 Å(*x*), 100 Å(*y*), and 126 Å(*z*). For COX-2, the grid box was centered at coordinates 29,926, 11,772, and 35,311 for the *x*, *y*, and *z* axes, respectively, with size parameters 112 Å(*x*), 80 Å(*y*), and 90 Å(*z*). For TRPA1 the grid box was centered on the entire enzyme with parameters 108Åx108Åx126Å and dimensions (*x*, *y*, *z*) = (161,851, 161,738, 157,285). Both Grids were centralized so that the protein chain was entirely within the computational simulation space. As criteria for preparing the protein structure, the methodology proposed by Yan et al. (2014), was used, where all water molecules were removed, and Gasteiger charges and essential hydrogen atoms were added. Preparation was performed using the ADT-AutoDocktools code (Morris et al. 2009).

Following the docking methodology proposed by Marinho et al. (2020), 50 independent simulations were performed, making it possible to obtain 20 poses per simulation both for docking and re-docking simulations and to improve the partial refinement of the individual calculations. of the couplings, the Exhaustiveness criterion was set to 64, keeping the protein structure was kept rigid, while all ligand bindings and twists were set to rotate (Nguyen et al. 2017). As a criterion for selecting the best pose, the statistical parameter RMSD (*Root Mean Square Deviation*) was used, with ideal values below 2 Å (Yusuf et al. 2008).

To evaluate the stability of the complexes formed in the simulations, the affinity energy (ΔG) was used, which has ideality parameters values lower than − 6.0 kcal/mol (Shityakov and Förster 2014). Using the affinity energy values,

the values of the inhibition constant (K1) (Eq. 2) of each complex were calculated (Kadela-tomanek et al. 2021).

$$\Delta G = -RTLnK \qquad (1)$$

$$Ki = e^{(\Delta G/RT)} \qquad (2)$$

ΔG is the binding free energy in KJ.mol-1, T is the absolute temperature, 298 K, R is the gas constant, 8.32 J. mol^{-1} K^{-1}, and Ki is the inhibition constant. To evaluate the strength of the H-bonds, the parameters proposed by Imberty et al. (1991), were used, which were based on the values of the distances between the donor and acceptor atoms, where the interactions were between 2.5 and 3.1 Å are classified as Strong, between 3.1 and 3.55 Å are considered Average and Weak those with a distance greater than 3.55 Å.

To validate the simulations, the re-docking technique was used. For the hypoglycemic activity, the co-crystallized α-acarbose ligand (PubChem CID: 445421) and the drugs Metformin (PubChem CID: 445421) and Miglitol (PubChem CID 441314) were used. For the anti-inflammatory activity, the co-crystallized ligands Flurbiprofen and Rofecoxib for COX-1 and COX-2 enzymes, respectively, and the drug Diclofenac (PubChem CID: 3033). The camphor antagonist (PubChem CID: 2537) was used as a reference for antinociceptive activity. All simulations of docking of reference drugs and re-docking of co-crystallized ligands were submitted to the same criteria and simulation conditions as the Chalcone.

In silico study of the pharmacokinetic properties of chalcone

Acidity, lipophilicity, and solubility

The two-dimensional structure of Thiophene Chalcone was designed to calculate ionization properties (pKa), partition coefficient (logP), distribution (logD) and solubility (logS) in Marvin JS, ChemAxon software (https://chemaxon.com/ products /marvin), as a method for predicting acidity, lipophilicity, and solubility attributes.

Multiparameter optimization (MPO) of ADMET Criteria

The physicochemical properties of molecular weight (MW), lipophilicity (logP), hydrogen bond acceptors, and donors and gyratory bonds (RB) were calculated using Marvin JS, ChemAxon software (https://chemaxon.com/products/marvin), and applied to the "rule of five" (Ro5) criteria updated by Lipinski in 2015 for space limitation of drugs with good oral bioavailability and interaction with biological targets (Lipinski 2016).

Physicochemical properties within the optimal drug-likeness threshold were converted into a quantitative

estimation drug-likeness (QED) score built into the ADMETlab 2.0 server (https://admetmesh.scbdd.com/) (Xiong et al. 2021), according to Eq. 3.

$$QED = \exp\left(\frac{1}{n} \sum_{n=1}^{n} \ln d_i \right) \qquad (3)$$

where the score ranges from 0 (poor toughness) to 1 (excellent toughness) for n properties evaluated within the ideal limit (d_i) (Bickerton et al. 2012).

The desirability of the permeability, efflux, and metabolic clearance pharmacokinetic parameters were estimated by the multiparameter optimization (MPO) technique inserted in the Marvin JS software, ChemAxon (https://chemaxon.com/products/marvin), based on the contributions of logP, logD, MW, polarity (TPSA), HB$_{don}$, and basic centers (pKa), converted to scores ranging from 0 (low desirability) to 6 (high desirability) (Wager et al. 2016).

Prediction of ADMET properties

To conduct the absorption, distribution, metabolism, excretion, and toxicity (ADMET) calculations, based on the methodology of Rocha et al. (2021), the molecule was subjected to the in silico filter of Brain Or IntestinaL EstimateD permeation (BOILED-Egg), built into the SwissADME server (http://www.swissadme.ch/), to predict intestinal and cerebral passive permeability through the lipophilicity (WlogP) and polarity (TPSA) descriptors, as well as P-glycoprotein (Pgp) substrates and nonsubstrates (Daina and Zoete 2016). While numerical parameters of apparent permeability (Papp) of colorectal adenocarcinoma cell (Caco2) and Madin−Darby canine renal cell (MDCK) cell models, plasma protein binding (PPB) and plasma−brain distribution (Cbrain/Cblood) were predicted by the in vitro and in vivo models of the PreADMET server (https://preadmet.bmdrc.kr/adme/).

The phase I metabolism of Chalcona was predicted by consensus testing of cytochrome P450 (CYP450) isoenzyme inhibitor and noninhibitor models (CYP450) from SwissADME and PreADMET servers. Although the possible CYP450 substrate sites were predicted on the SOMP Online server (http://www.way2drug.com/SOMP/) (Rudik et al. 2015).

For prediction of toxic effects, the main Chalcone microspecies and the metabolite formed by first-pass metabolism were submitted to the PASS Online server (http://way2drug.com/PassOnline/) (Filimonov et al. 2014) for acidosis models metabolism, sensitization, hepatotoxicity and liver damage.

ALARM NMR screening

Structural contributions were detected through the high-throughput screening method (HTS) of a La assay to detect reactive molecules by nuclear magnetic resonance (ALARM NMR), built into the ADMETlab 2.0 web server (https://admetmesh.scbdd.com/) (Xiong et al. 2021).

Inhibition of target classes, biological activity, and acute oral toxicity

The substance was submitted to the QSAR applicability domains of the GUSAR Online server, Way2Drug (http://www.way2drug.com/gusar/index.html), to predict the inhibition of models of biological receptors, enzymes and active transporters and determination of the lethal dose (LD50) through quantitative regression of the electrotopological neighborhood of atoms (QNA). While biological and microbial activities were predicted by similarity testing of the in vivo animal test dataset from the PASS Online server (http://way2drug.com/PassOnline/) (Lagunin et al. 2011; Filimonov et al. 2009).

Results and discussion

With emphasis on the structure of chalcone and the number of replaceable hydrogens, the possibility opens up for derivative synthesis with different functional groups that result in various biological activities such as anticancer (Chavan et al. 2023), antidiabetes (Rocha et al. 2020), anxiolytic (Ferreira et al. 2020) and anticonvulsants (Ferreira et al. 2018; Mendes et al. 2022). The synthesis by the Claisen−Schmidt condensation reaction aims to obtain medium to high yield chalconic derivatives (Bandeira et al. 2019; Kumar et al. 2022), and still uses environmentally-friendly solvents (Clarke et al. 2018). Aiming at the application as a possible drug, the well-defined synthesis of the compound is necessary for use on a large scale.

^{1}H NMR showed peaks at δ_H 3.92 (s), and 4,03 (s) for synthesized chalcone, these peaks corresponding to hydrogen atoms from three methoxy groups. The peak at δ_H 5.97 (s), and 6.08 (s) is due to the only hydrogen atom bound to the aromatic ring for both chalcones. In addition, the peaks 7.78 (d, $J = 15.3$ Hz), and 8.01 (d, $J = 15.3$ Hz) were attributed to doublets referring to α, β unsaturated hydrogens. ^{13}C NMR revealed in ring A five aromatic quaternary carbon atoms with peaks at δ_C 159.6 (C-4'), 158.6 (C-6'), 158.8 (C-2'), and 131.1 (C-3') and 107.0 (C-1'), and only one aromatic methine carbon at 87.3 (C-5'). In addition, it was possible to observe a signal concerning to α, β unsaturated carbonyl at δ_C 192.7 ppm. The olefinic carbons are observed at 126.6 (Cα) and 131.8 (Cβ), respectively. The signals at
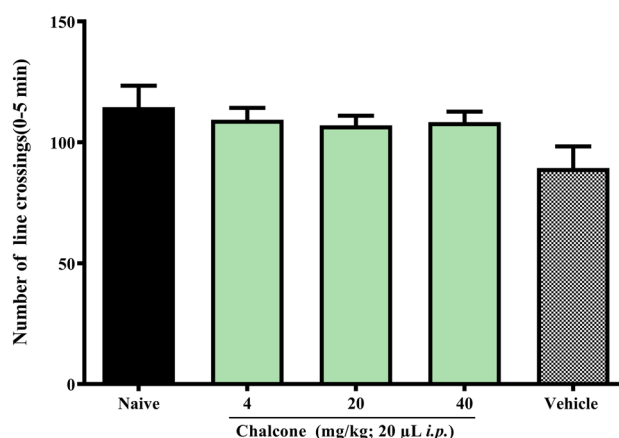

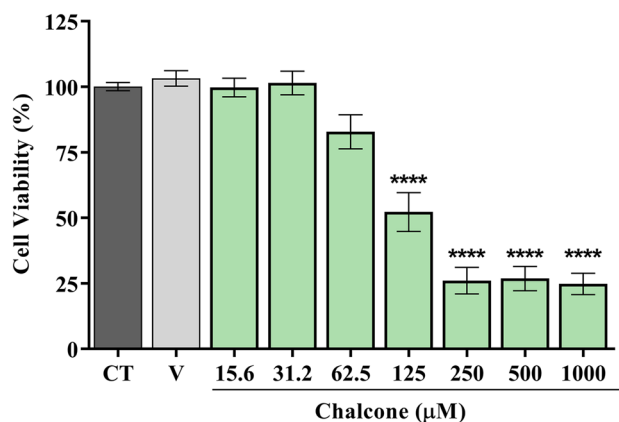**Fig. 1** Effect of chalcone on zebrafish locomotion in the open field test (0-5 min)

Fig. 2 Chalcone cytotoxicity in PC12 cells by MTT assay. Results are expressed as the percentage of damaged cells ± S.E.M. *$p < 0.05$ vs. control group; V – vehicle group (DMSO 0.5%)

δ_C 56.1−61.0 refer to the carbons of the methoxy groups and the peaks at δ_C 141.3 (C-1), 135.6 (C-5), 131.7 (C-4) and 128. 6 (C-3) refer to the carbons of the thiophene ring.

Chalcone was not toxic in adult zebrafish during the 96 h analysis ($LD_{50} > 40.0$ mg/kg). Furthermore, it did not change the locomotion of adult zebrafish in the open field test, as all doses showed locomotor activity significantly (p ˃ 0.05), similar to that of the naive group (Fig. 1). In the previous works, it weas showed that other chalcones, also from the same natural product, did not show toxicity under the same conditions used in this work (Ferreira et al. 2021).

According to Fig. 2, chalcone showed no cytotoxicity in the concentration range from 15.6 to 62.5 μM. However, at higher concentrations, there was a reduction in the percentage of viability of PC12 cells, differing statistically from the control with (p > 0.0001). In experimental models of neurotoxicity and neuroprotection in vitro, PC12 cells are

widely used due to their good correlation with in vivo assay (Yang et al. 2017; Chen et al. 2022). These results are in agreement with the findings by Mendes et al. (2022), which showed that a heterocyclic chalcone (*E*)-3-(furan-2-yl)-1-(2hydroxy-3,4,6-trimethoxyphenyl)prop-2-en-1-one), derived from same acetophenone also showed low toxicity. Therefore, our results indicate that this molecule has a low cytotoxic effect, which makes it viable to be explored in new experiments. After performing the toxicological tests, the pharmacological tests continued.

The zebrafish has emerged over the past 3 decades as an ideal animal model for studying the basic events that lead to embryonic development and for modeling human disease. Thus, animal models of nociception are critical to understanding the biological processes associated with pain and their significant effects on behavior, as highlighted by Costa et al. (2022) when addressing behavioral phenotypes related to nociception in adult zebrafish. In the formalin-induced nociception model, it was observed that chalcone at the dose (10 mg/kg) and morphine reduced ($p < 0.0001$ vs. Control) the number of formalin-induced nociceptive behaviors in the neurogenic phase (Fig. 3A), while all doses of chalcone as well as morphine inhibited ($p < 0.0001$ vs. Control) the

behavior of animals in the inflammatory phase (Fig. 3B). When investigating the mechanism of antinociceptive action, camphor was used, which acts on the transient ankyrin receptor potential 1 (TRPA1) channel preventing analgesia. Therefore, it was possible to notice a decrease in the locomotor behavior of the animals at the dose of 40 mg/kg only in the second phase (****$p < 0.0001$ vs. control; Fig. 3B). And so, it was deduced that chalcone could modulate the TRPA1 channel in the inflammatory phase. Previous findings show that the nociceptive effect was also reversed by 3,4-dihydroxychalcone (Heidari et al. 2009) and natural dimeric chalcones extracted from *Myracrodruon urundeuva* (Viana et al. 2003).

When performing Molecular docking simulations of the chalcone with the TRPA1 channel (Fig. 4), it was possible to observe that all simulations presented RMSD (Root Mean Square Deviation) value within the ideal parameter, less than 2 Å (Yusuf et al. 2008), in the case of chalcone it presented a value of 1581 Å and camphor antagonist in the order of 1892 Å. The Chalcone−TRPA1 complex presented energy in the order of − 6.0 kcal/mol and the camphor−TRPA1 complex in the order of − 5.4 kcal/mol. The inhibition constants were 3979×10^{-5} (pKi = 4.40), 1096×10^{-4} (pKi = 5.72) for
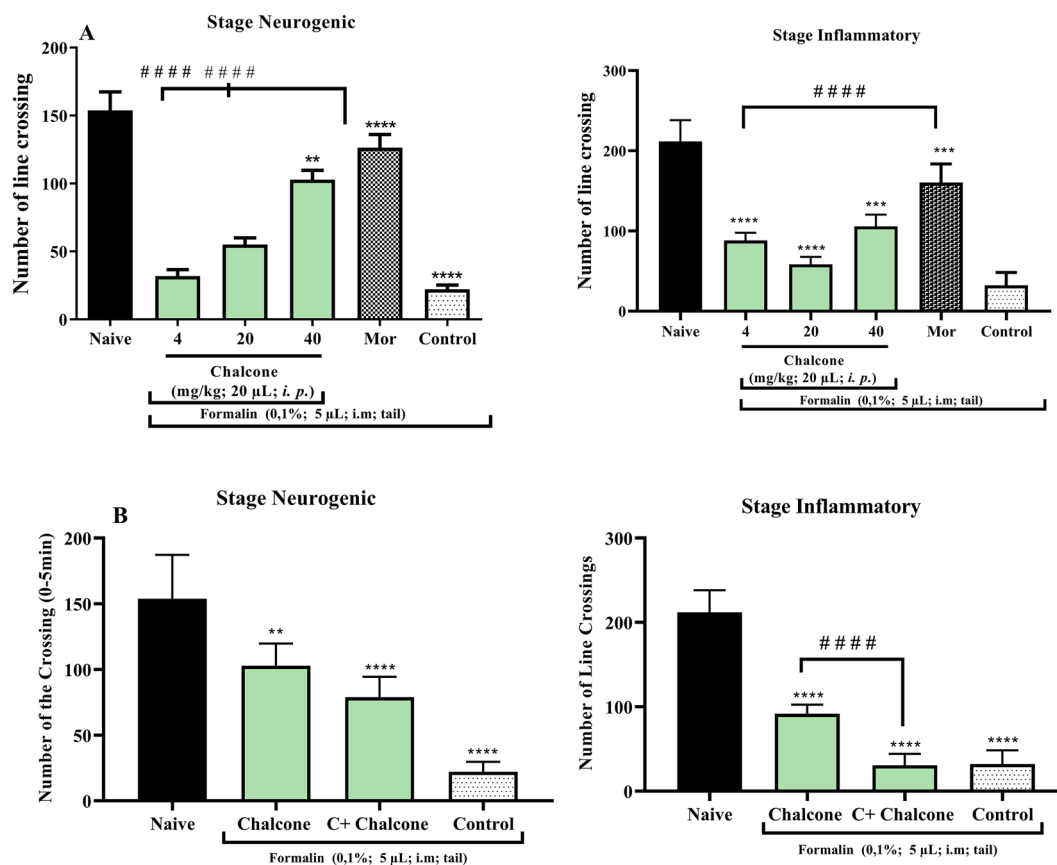

Fig. 3 **A** Antinociceptive activity of chalcone by formalin model in adult zebrafish (Danio rerio). **B** Antinociceptive mechanism of action of chalcone induced by formalin in adult zebrafish (Danio rerio)
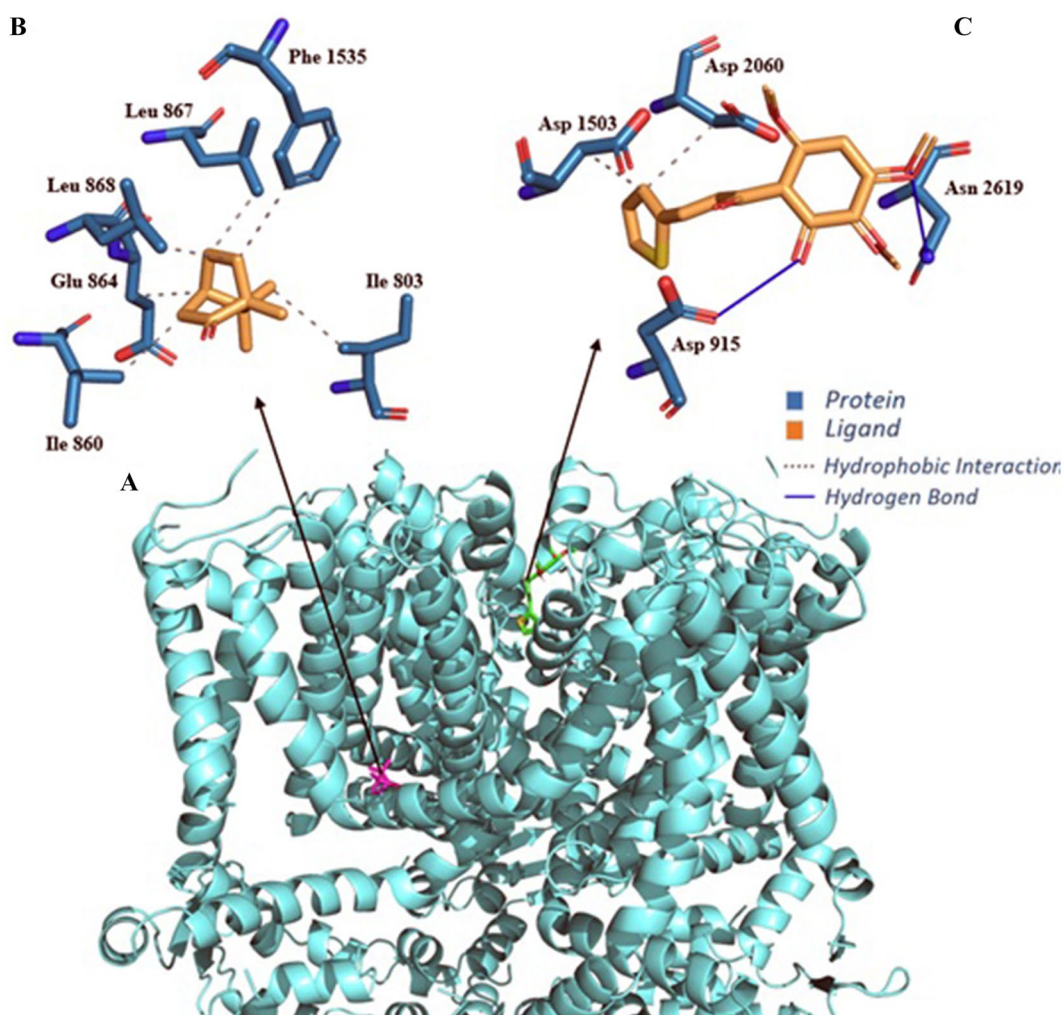
Fig. 4 Human TRPA1 receptor interaction complex with ligands (**A**); Interaction maps of camphor antagonist (**B**) and chalcone ligand (**C**)

the Chalcone−TRPA1 and camphor−TRPA1 complexes, respectively (Table S1, supplementary material). Analyzing the chalcone−TRPA1 complex, four interactions are verified: two hydrophobic with residues Asp 1503 B (3.81 Å) and Asp 2060 C (3.82 Å) and two H-bond with residues Asp 915 A (2.64 Å) and Asn 2619 D (3.07 Å). Notably, the complex formed by the antagonist camphor with TRPA1 is formed by six hydrophobic interactions involving residues Ile 803 A (3.64 and 3.96 Å), Leu 863 A (3.54 Å), Glu 864 A (3.65 Å), Leu 867 A (3.20 Å) and Phe 1535 B (3.71 Å) (Table S2, supplementary material).

Given the reversal of the nociceptive behavior of animals in the inflammatory stage after pre-treatment with chalcone, the anti-inflammatory activity of chalcone was investigated in vitro through its ability to inhibit the production of nitric oxide (NO), stimulated by lipopolysaccharide (LPS), in J744A.1 macrophages. In this sense, it is worth mentioning that NO is involved in critical physiological processes such as neurotransmission, mitochondrial respiration,

gastric motility, and inflammation (Lo Faro et al. 2014). However, NO overexpression contributes to inflammatory processes promoting vascular permeability and leukocyte infiltration (Nagy et al. 2008). The results showed that the effect of chalcone on the viability of J774A.1 murine macrophage cells showed cytotoxicity with IC_{50} values between 12.91 ± 1.32 µM. In addition, chalcone was evaluated for its inhibitory effect on NO production in LPS-activated J774A.1 cells (Fig. 5). Thus, chalcone effectively inhibited NO production. However, it was not possible to calculate the IC_{50} value of the samples against the inhibition of the production of NO by the results found, where there was no difference in response between the concentrations used.

In zebrafish, the anti-inflammatory activity of chalcone was performed by the carrageenan-induced abdominal inflammation model. As shown in Fig. 6, the anti-inflammatory effect of chalcone (40 mg/kg) reduced ($P < 0.01$) abdominal edema corresponding to the positive control ibuprofen ($P < 0.001$; 100 mg/kg). In terms of structure−activity

Fig. 5 Effect of chalcone on the viability of J744A.1 cells (**A**). Effect of chalcone on the inhibition of NO production in LPS-stimulated J744A.1 cells (**B**)
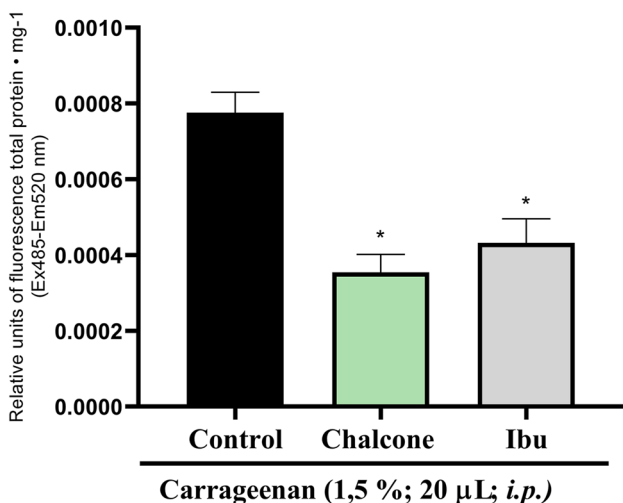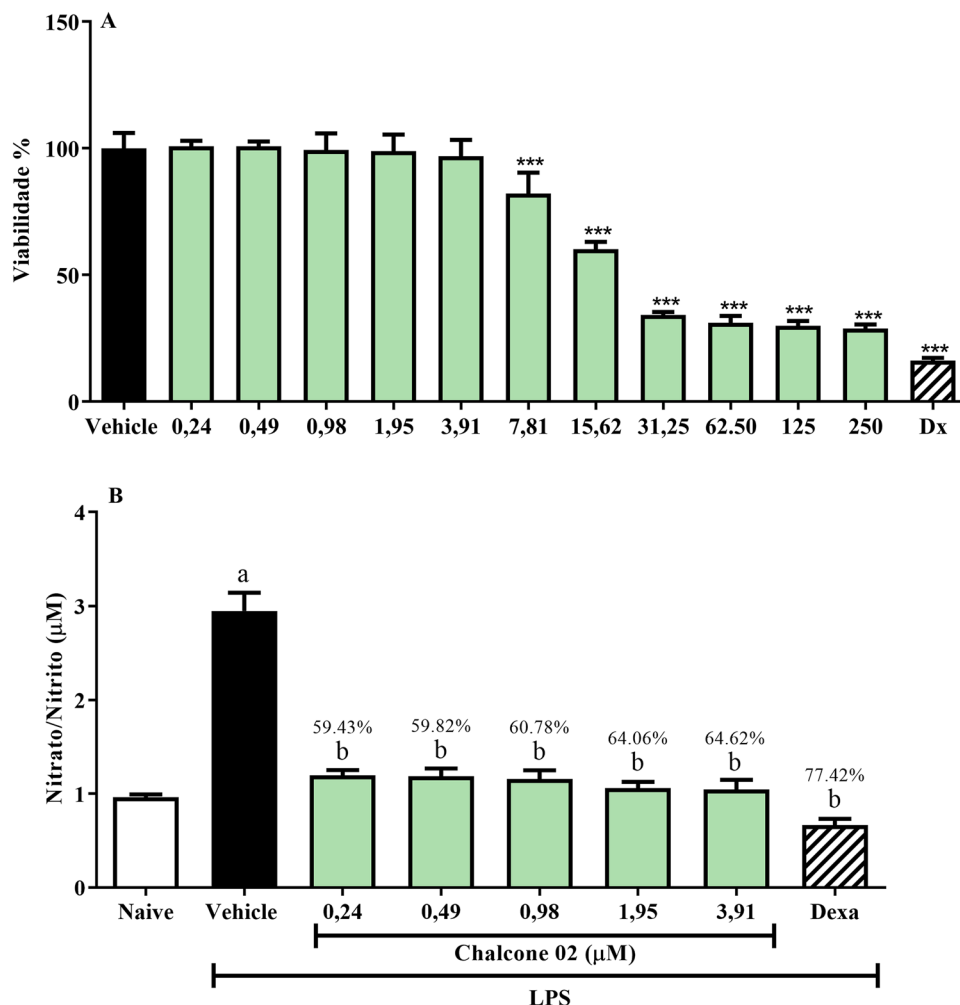

Huang et al. (2020), when performing a screening of chalcone analogues with antidepressant, anti-inflammatory, analgesic and COX-2 inhibitor effects, found that compounds with electron-donating substituents also showed anti-inflammatory activity compared to the control group with the following activity order: 4-OH > 4-CH(CH$_3$)$_2$ > 3-OCH$_3$ > 2—CH$_3$ > 4-N(CH$_3$)$_2$ > 3-CH$_3$ > 4-OCH$_3$ > 3-OH-4-OCH$_3$ > 3-OH > 2-OCH$_3$ > 4 -CH$_3$. Likewise, the chalcone structure of this work also presents 2 of the electron-donating substituents present in the chalcone analogues with anti-inflammatory activity: -OH e -OCH$_3$.

Inflammation comprises multiple processes involving the activation of inflammatory cells, the secretion of pro-inflammatory cytokines and the release of different inflammatory mediators, including PGE$_2$ and COX-2. For example, COX-2 is involved in the production of the inflammatory mediator PGE$_2$, which results in the symptoms of inflammation, such as redness, swelling, fever, and pain. (Ou et al. 2019). Carrageenan-induced abdominal edema in adult zebrafish is a well-defined model of inflammation for the study of natural and synthetic anti-inflammatory products (Batista

Fig. 6 Liver oxidative stress after induced inflammation in zebrafish

et al. 2018; Huang et al. 2014). The recent research has indicated that chalcones derivatives may inhibit the secretion of phospholipase A2, COX, and pro-inflammatory cytokines (Tang et al. 2020).

In an inflammatory condition, immune cells release ROS leading to oxidative stress (Hussain and Harris 2007; Reuter et al. 2010). Regarding the effect of chalcone on oxidative stress in liver tissue after induction of abdominal edema, a reduction in ROS levels of liver tissue from swollen zebrafish can be observed (* $p < 0.05$, vs. control; Fig. 7).

This result indicates that the inflammatory response induced by Carrageenan was closely related to the reduction of antioxidant enzyme activities and the generation of free radicals and lipid peroxidation, which has been shown to control the redox state in the liver after inflammation (Lai et al. 2009). In view of these results, molecular docking simulations were used to study the probable binding mode of chalcone at the active site of COX-1 and 2.

Coupling simulations with Cyclooxygenase-1 (COX-1) and 2 (COX-2) indicated that chalcone has a greater
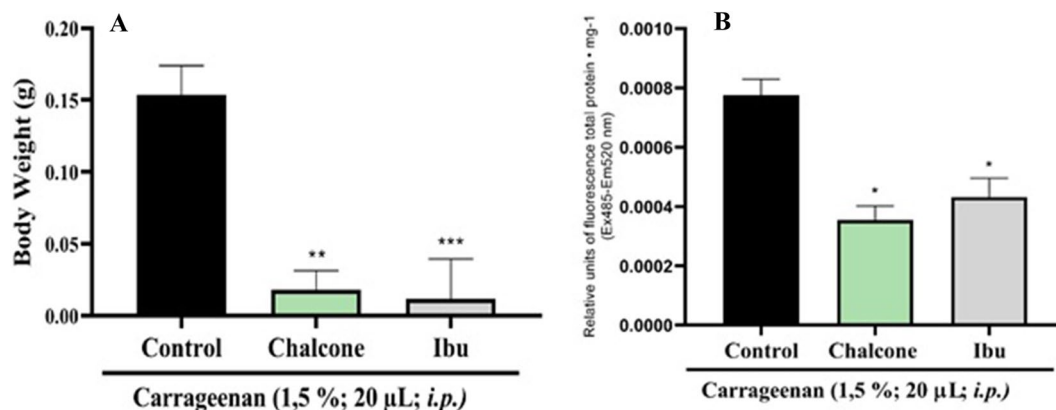

Fig. 7 Anti-inflammatory effect of chalcone on adult zebrafish (Danio rerio) (**A**); Effect of chalcone on liver tissue oxidative stress induced by abdominal edema (**B**)
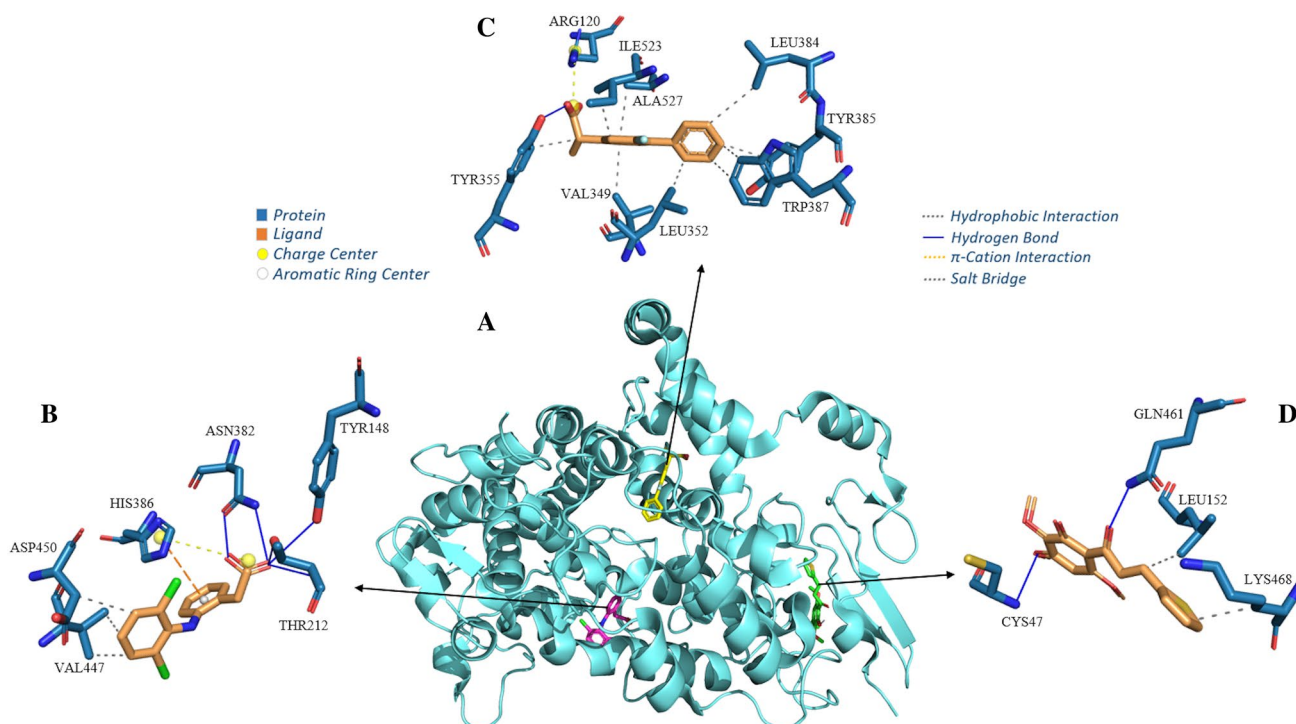

Fig. 8 Cyclooxygenase-1 enzyme interaction complex with ligands (**A**); Interaction maps of the drug Diclofenac (**B**), the co-crystallized inhibitor Flurbiprofen (**C**) and the ligand Chalcone (**D**)

affinity for the COX-1 enzyme (Fig. 8), as it presented affinity energy in the order of − 7.1 kcal/mol for Cox-1 and -5.8 kcal/mol for COX-2. What can be seen is that the chalcone−COX-1 complex, when compared with the Flurbiprofen−COX-1 complex calculated by re-docking (− 6.5 kcal/mol), also showed a higher affinity, which is also valid when compared with o the energy of the Diclofenac−COX-1 complex (− 5.9 kcal/mol). This affinity can be better analyzed through ki and pKi, where it can infer that chalcone will need a lower concentration than diclofenac and flurbiprofen to inhibit COX-1 (Table S1, supplementary material). Furthermore, regarding the positioning of the ligands in COX-1, it can infer that chalcone, flurbiprofen and diclofenac couple in different regions. Moreover, when analyzing the formation of the Chalcone−COX-1 complex, it is possible to highlight two hydrophobic interactions, one in the order of 3.97 Å with the side chain of the aliphatic residue Leu 152B and another in the order of 3.47 Å with the basic residue LYS468B.

The hydrophobic interactions between chalcone and the amino acid residues of the COX protein occur because of the molecular skeleton of carbon (the phenyl ring, the thiophene ring, and the olefin double bond) have a partial negative charge spread over them. Therefore these π electrons can be donated to the residue, or they can be used to accept the electron density of the residue using the empty $\pi*$ antibonding molecular orbitals. Analyzing the structure of the molecule, the importance of oxygen atoms is also highlighted, which contribute as acceptors, resulting in two H-bond atoms, one of 2.09 Å with an important acidic H-bond chain Gln 461B and the other on the order of 3.00 Å with the side chain of the polar residue Cys 47B. Furthermore, as seen in Fig. 7, oxygen atoms have a higher concentration of negative charge that can be used to form strong H bonds (Table S3, supplementary material).

When comparing the complex formed by the chalcone with the COX-2 enzyme and the co-crystallized ligand (Rofecoxib) and the reference drug (diclofenac), it can be observe that the complex Rofecoxib-COX-2 and Diclofenac-COX-2 present a more favorable affinity energy than the Chalcone−COX-2 complex, indicating that a higher concentration of chalcone will be required than diclofenac and Rofecoxib to inhibit COX-2 (Table S4, supplementary material). Furthermore, by observing the coupling site, it is possible to observe that Diclofenac couples in the same region as Rofecoxib, inferring that the action of diclofenac is preferential via COX-2 (Fig. 7B).

Inflammation is already proven to be a major risk factor for type 2 diabetes, atherosclerosis, cancer and other chronic diseases (Kaur and Singh 2022; Rohm et al. 2022). Inflammatory responses may establish a causal relationship in the onset of DM2, which further contributes to insulin resistance, or may increase through the hyperglycemic state that leads to the complications of DM2. (Halim and Halim 2019). In order to evaluate the hypoglycemic effect of chalcone, acute and chronic hyperglycemia was induced by sucrose.
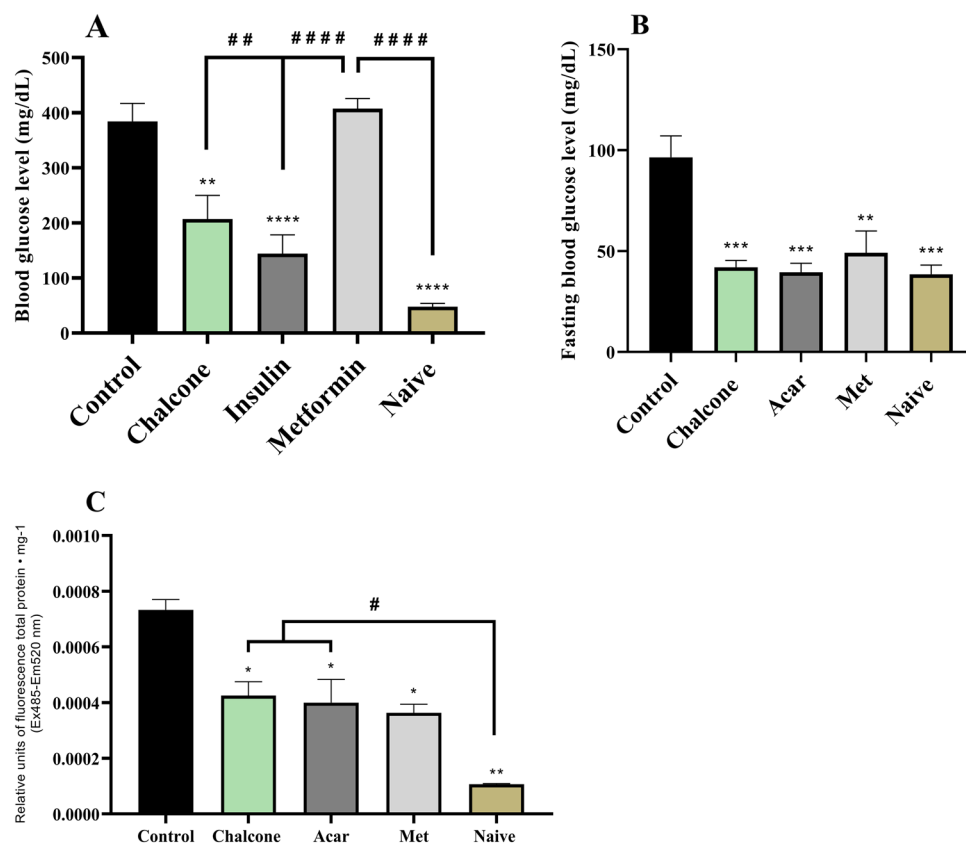
To date, this is the first work with a model of sucrose-induced acute hyperglycemia, which in turn caused (****$p < 0.0001$ vs Naive) an increase in the acute glycemic index in animals (Fig. 9A). This hyperglycemic effect was reduced (****$p < 0.0001$ vs Control) by insulin at baseline levels similar to the Naive (no treatment) group. The drug metformin hydrochloride did not reduce acute hyperglycemia. Chalcone (40 mg/kg) reversed (**$p < 0.01$ vs Control) sucrose-induced acute hyperglycemia. Thus, this result shows that the model allows the investigation of the impact of acute hyperglycemia in animals to study the physiological processes altered by this disorder.

The previous research shows hyperglycemia induced by high sucrose concentration (83.25 mM) for 14 days, and the effects analyzed were related to learning and memory in zebrafish (Ranjan and Sharma 2020). It was observed that sucrose caused hyperglycemia in Zebrafish from the fourth day of induction. Therefore, the same procedure was performed to induce hyperglycemia in adult Zebrafish by immersion in sucrose at 83.25 mM for seven days. With sucrose withdrawal after four days, the persistence of hyperglycemia (***$p < 0.001$ vs Naive) was observed after 12 h of fasting in the control group (3% DMSO) (Fig. 9B.). The persistence of sucrose-induced hyperglycemia was significantly reduced (**$p < 0.01$ vs Control) by chalcone (40 mg/kg) (Fig. 9B), an effect similar to positive control groups (Sugar—Acarbose and Met—Metformin) that reduced (**$p < 0.01$; ***$p < 0.001$ vs Control) hyperglycemia to baseline levels in animals.

The basal fasting blood glucose level in zebrafish is approximately 50–75 mg/dL (Jörgens et al. 2012), a result similar to that obtained in this study with untreated animals (Naive) after 12 h of fasting. Capiotti et al. (2014) induced hyperglycemia in adult Zebrafish with glucose at 111 mM for 14 days and observed the persistence of hyperglycemia after seven days of glucose withdrawal, suggesting that exposure of these animals to high concentrations of glucose is capable of inducing persistent metabolic changes, likely determined by a hyperinsulinemic state and impaired peripheral glucose metabolism.

Sucrose-induced hyperglycemia increased (***$p < 0.001$ vs Naive) the levels of reactive oxygen species in the liver of the animals. However, oxidative stress was significantly reduced (*$p < 0.05$ vs Control) by chalcone (Fig. 9C), an effect similar to positive control groups (Sugar—Acarbose and Met—Metformin; *$p < 0.05$ vs Control). Therefore, the results showed that the persistence of sucrose-induced hyperglycemia was significantly reduced (**$p < 0.01$ vs Control) by chalcone.

Fig. 9 Effect of chalcone on acute (**A**) and chronic (**B**) hyperglycemia and liver oxidative stress induced by chronic hyperglycemia (**C**)

The literature shows that chalcones have a hypoglycemic effect by acting on different targets, such as: inhibiting carbohydrate digestion, aldose reductase to increase GSH synthesis, inhibiting cellular sorbitol-mediated osmotic pressure and reducing the production of end products of advanced glycation (AGEs), activate the transactivation potential of erythroid-derived nuclear factor 2 (Nrf2) to enhance antioxidation, detoxification, and cytoprotection, inhibit *Sodium-Glucose Co-Transporter* (SGLT-2) reabsorption, and ultimately mimic insulin, thereby lowering the blood glucose level (Adelusi et al. 2021). The antidiabetic properties of chalcones have been well reported (Rocha et al. 2020).

The high glycemic content in diabetes mellitus 2 stimulates the generation of ROS, which still play a vital role in developing comorbid conditions, such as insulin resistance, hyperlipidemia, inflammation, and oxidative stress (Rout et al. 2021). This is due to a decrease in the decomposition and/or an increase in the production of antioxidants such as catalase (CAT—enzymatic/nonenzymatic), superoxide dismutase (SOD) and glutathione peroxidase (GSH-Px). As a result, changes in the levels of these enzymes make tissues susceptible to oxidative stress, leading to diabetic complications (Lipinski 2004). It is for this reason that the persistence of chronic hyperglycemia after sucrose withdrawal caused oxidative stress in the liver and brain tissue of the animals (Fig. 9C). However, treatment for four days

with chalcone (40 mg/kg) protected liver tissue from ROS produced by sucrose-induced hyperglycemia. Chalcones are known for their free radical scavenging properties through the hydrogen atom transfer (HAT) mechanism. Their ability to remain stable after donating these hydrogen atoms is due to the delocalized π electrons hovering around their aromatic structures (Adelusi et al. 2021).

One of the strategies explored by chalcones and other natural products on diabetes and its complication is the inhibition of carbohydrate digestion. Pancreatic α-amylase and intestinal α-glucosidase are the two key enzymes responsible for carbohydrate digestion, and their ultimate effect is postprandial hyperglycemia. As a result, complex carbohydrate starches are hydrolyzed by pancreatic α-amylase into oligosaccharides, while these oligosaccharides are hydrolyzed into monosaccharides by intestinal α-glucosidase, thereby increasing the blood glucose level (hyperglycemia) – a condition closely linked to diabetes (Adelusi et al. 2021). This is why postprandial glucose levels are controlled by α-glucosidase inhibitors, a class of antihyperglycemic drugs that are often given to individuals with type 2 diabetes (Adelusi et al. 2021). Therefore, using the computer simulation technique (molecular docking), it was possible to obtain a structural view of the mechanisms of inhibition of ligands on α-glucosidase, identifying the modes of interaction of the ligand with the active site of the protein.

After choosing the best pose, with the lowest RMSD value and affinity energy as parameters, it was possible to observe that chalcone has more favorable energy than the reference drugs miglitol and metformin, as it presented lower affinity energy (− 6.2 kcal/mol). However, it was less favorable when compared with α-acarbose, which presented energy in the order of − 7.9 kcal/mol. This analysis can be refined when evaluating the inhibition constant (Ki) and pKi, where it can be inferred that the lower the Ki value, and the higher pKi, the greater the affinity of the ligand for the protein and, consequently, the lower the concentration of ligand required to inhibit enzyme activity (Kadela-tomanek et al. 2021). From this perspective, it is possible to infer that chalcone will need a lower concentration to inhibit CtMGAM than miglitol and metformin, since it presented lower ki, in the order of 2.893×10^{-5}, a higher pKi value (4.54), and a higher concentration when compared with the co-crystallized inhibitor (α-acarbose) which presented Ki and pKi in the order of 1.904×10^{-6} and 5.72 respectively (Table S1, supplementary material).

However, it can be observed that the chalcone−CtMGAM complex is formed by four H-bonds, two of which are moderate, involving the chalcone oxygen atoms (acceptors) with the nitrogen (donor) present in the primary amino acid residue of the ARG1730 of the A chain, and two bonds involving the oxygen atoms (acceptor) of the chalcone with H-bond−bond donor atoms of the residues GLN 1731 A and TYR 1787 A. The chalcone still forms a hydrophobic interaction with the residue HIS 1730 A and a π-Stacking involving the side chain of residue HIS 1727 A. Furthermore, it is observed that metformin complexes in the same region of the α-acarbose site, where the interaction with residue ASP 1526 A stands out, forming salt bridges with the metformin and H-bond with α-acarbose. Also noteworthy is the residue ARG 1510 A, which forms a strong H-bond with metformin and the α-acarbose ligand. It can be observed that miglitol complexes in a different region from metformin and chalcone, complexing with H-bond bonds, where the acidic side chain residue GLU1400A stands out, which interacts forming five strong interactions, with a distance varying from 2.27 to 3.04 Å (Table S2, supplementary material). Therefore, when is analyzed the formation of complexes, it is possible to observe that chalcone complexes in a different site from metformin and α-acarbose, which are complex in the same region (Fig. 9B) and from miglitol, indicating that chalcone does not compete by the site of interaction of these drugs, thus indicating the possibility of synergistic use of chalcone with these reference drugs (Fig. 10).

The use of computational techniques in the prospection of new drugs can reveal those with better therapeutic efficacy. A study was carried out by the ADMET profile (Adsorption, Distribution, Metabolism, Excretion, and Toxicity), which provides results that can be channeled to further studies, whether in vitro, in vivo or clinical studies. Regarding the main microspecies, lipophilicity and solubility of the molecule: The most acidic pKa value
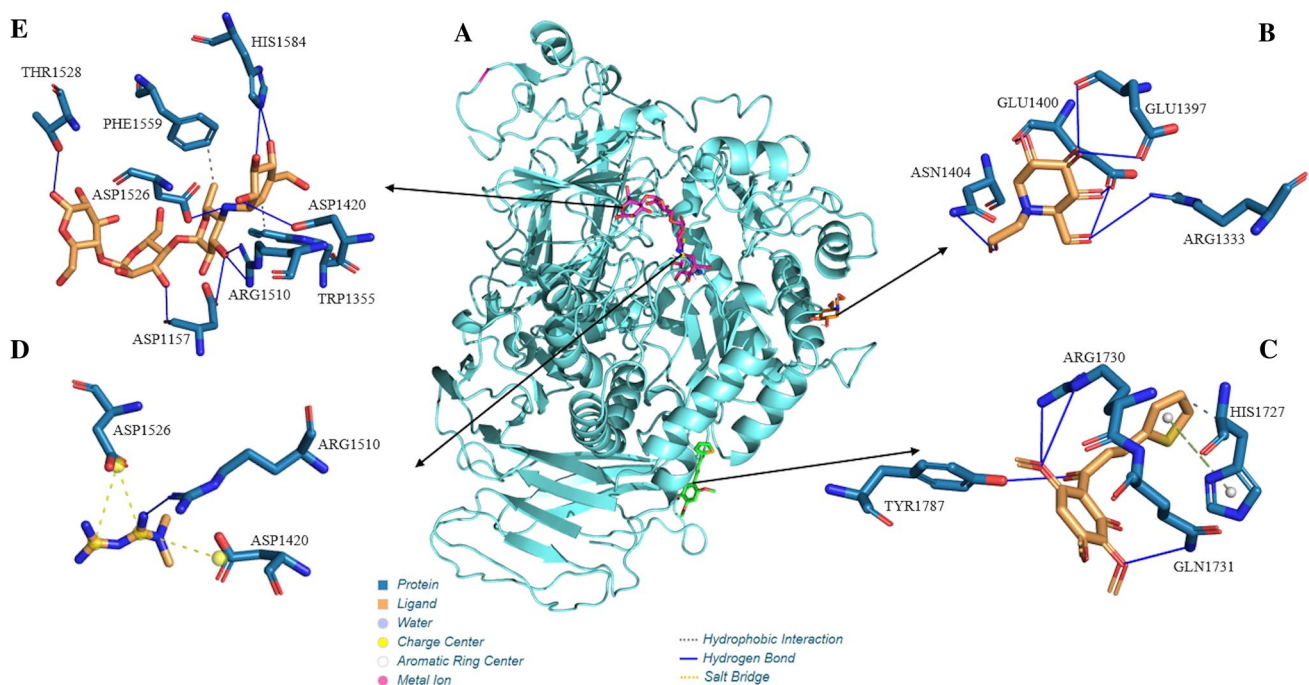

Fig. 10 Interaction complex of the enzyme CtMGAM with the ligands (**A**); Interaction maps of the ligand miglitol (**B**), chalcone (**C**), the drug metformin (**D**) and the co-crystallized inhibitor alpha-acarbose (**E**)
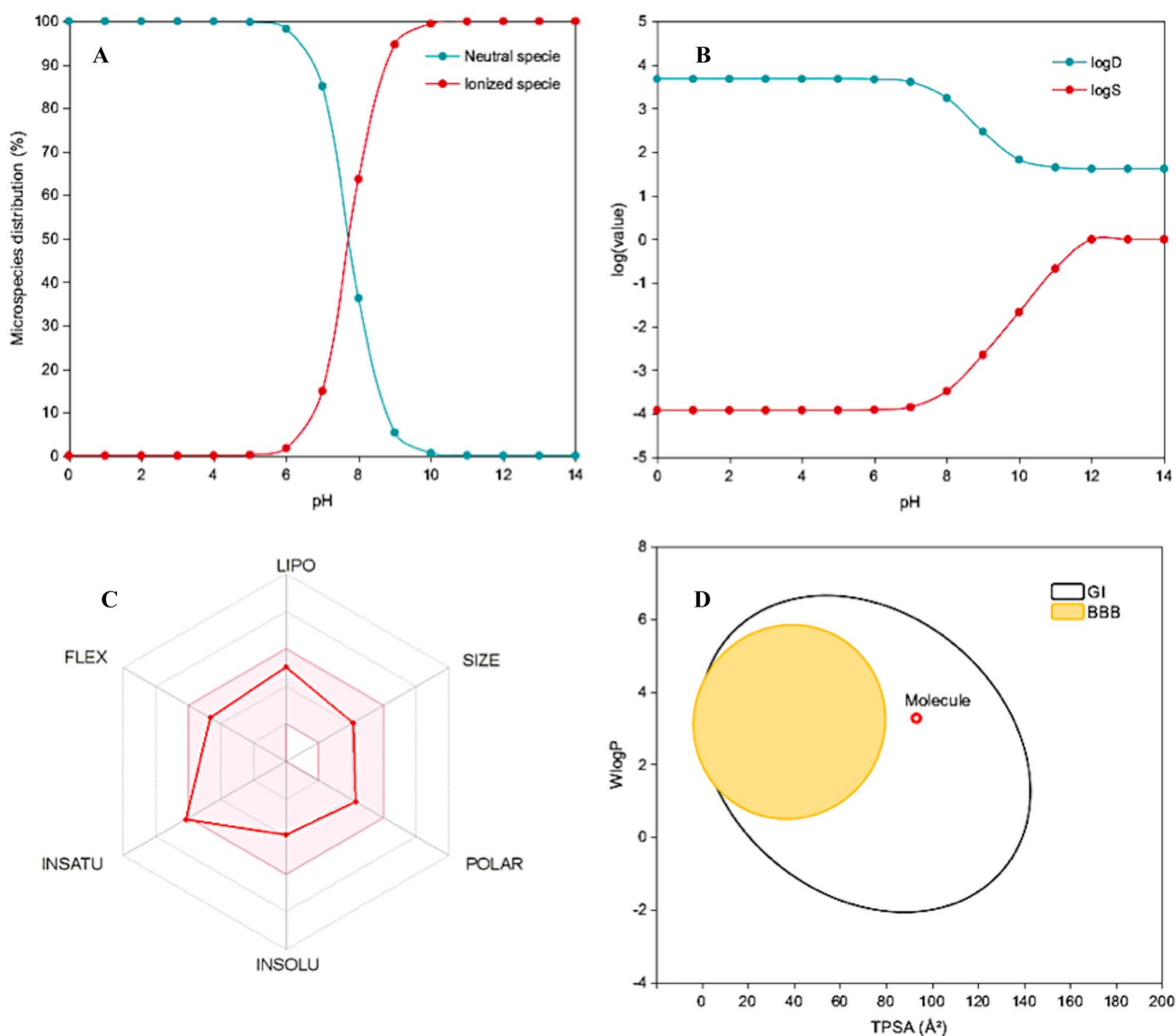
Fig. 11 **A** Distribution of microspecies, **B** distribution and solubility coefficients as a function of pH variation, **C** Bioavailability radar with physicochemical limits and **D** Boiled egg graph for intestinal prediction (HIA) and cerebral permeation (BBB) of chalcone

evaluated at 7.76, a value compatible with other hydroxyl groups, suggests the presence of an ionized molecular fraction at physiological pH (approximately 7.4), with an approximate concentration of 30% as shown in the graph of Fig. 11A. This is an essential finding for oral bioavailability since hydrogen donor groups decrease the chalcone volume of distribution. The graph in Fig. 11B shows a decrease in the Chalcona distribution coefficient, which shifts the chemical equilibrium towards increasing solubility. Thus, it is possible to observe the variation in the lipid solubility of the substance with the decrease in the molecular volume of the neutral microspecies as a function of the pH variation. The calculated value of logD in the order of 3.52 suggests that the levels of lipophilicity of

the molecule guarantee a balance between solubility and permeability (Fichert et al. 2003).

An analysis of the physicochemical properties of chalcone on the bioavailability radar of Fig. 11C shows that the substance is within the limits of size (MW < 500), lipophilicity (log P < 5) and flexibility (N_{RB} < 10) established by the criteria of Ro5, satisfying the conditions established for its use as an oral medication. As a general rule of thumb, a substance has good oral bioavailability when it is uncharged and not as lipophilic (Salah et al. 2016; Khan et al. 2018). The evolution of Lipinski's "rule of five" (Ro5) in 2015 considers a space of physicochemical properties where there is a probability that a compound has good oral bioavailability, and that coincides with structural limitations of

interaction with protein targets, which include: MW < 500 g/mol, log$P$ < 5, hydrogen bond acceptors (HB$_{Acc}$) < 10, hydrogen bond donors (HB$_{Don}$) < 5 and spinner bond number < 10 (Lipinski 2016). Optimal properties within established limits are converted into a quantitative estimate of drug-likeness (QED) score, as per Eq. 1. Higher values (on a scale of 0 to 1) are associated with better plasma clearance, plasma free fraction, half life and elimination, as key pharmacokinetic attributes (Bickerton et al. 2012).

It is interesting to note that chalcone exceeds unsaturation levels (Fsp3 < 0.25), with 2 aromatic rings, while the presence of a hydrogen donor atom, associated with phenolic hydroxyl, suggests the formation of ionized microspecies in specific ranges of physiological pH, factors that limit its drug ability. However, the QED value evaluated at 0.65 suggests that most of the physicochemical properties of Chalcona satisfy the ideal drugability parameters. At the same time, the CNS MPO score in the order of 4.65 indicates a high permeability, low passive efflux and low probability of access to CNS, favorable pharmacokinetic attributes for good oral bioavailability (Table S5, supplementary material).

An essential application of desirable pharmacokinetic indices is associated with multiparameter optimization of central nervous system drugs (CNS MPO). The limits of six of these parameters include logP ≤ 3, logD ≤ 2, MW ≤ 360, HB$_{don}$ ≤ 1, TPSA ≤ 90, and the most basic pKa ≤ 8, which guarantee a physical−chemical space that favors the three fundamental attributes of ADMET: high permeability, low passive efflux and low metabolic clearance, as well as ensuring safe access to the central nervous system. Thus, CNS MPO scores > 4 are associated with compounds well absorbed in the human intestine, and blood−brain barrier (BBB) permeability tends to approach 6 (Wager et al. 2016) (Wager et al. 2010).

As physicochemical properties are dependent on molecular size and the presence of hydrogen acceptors and donors, the evaluated lipophilicity and polarity profiles of Chalcone plotted on the BOILED-Egg plot in Fig. 11D show that the substance has high passive gastrointestinal permeability, as it is within the limit formed by the TPSA intervals lower than 142 Å^2 and logP between −2.3 and 6.8, with a Papp coefficient in the order of 3.32×10^{-6} cm/s, and is not a substrate of Pgp, which guarantees a good bioavailability after human intestinal absorption (HIA) (Yee 1997). However, the substance does not have activity in the central nervous system (CNS), as the TPSA > 79 Å^2 and the Papp coefficient in the order of 1.13×10^{-5} cm/s suggest a low passive permeability in the BBB, where the percentage of binding with plasma proteins on the order of 90.27% result in a C$_{brain}$/C$_{blood}$ distribution of only 0.01 (Silverman and Holladay 2014) (Table S6, supplementary material).

In the prediction of first-pass metabolism, the servers pointed to a potential inhibition of Chalcone to the CYP2C19 and CYP2C9 isoenzymes, suggesting an increase in the concentration of the substance in the blood plasma, as well as an ambiguous behavior with the CYP3A4 isoform (Table S6, supplementary material). The predictions also showed that the methyl group of p-OCH3 is likely to be a substrate site of CYP2D6 with a probability of approximately 80%, through a hydroxylation reaction followed by demethylation, resulting in a p-OH type substitution as shown in Scheme S1 (supplementary material). Consequently, the formed metabolite has a decreased probability of metabolic acidosis, sensitization and liver toxicity, and an increased probability of liver toxicity to the generic structure. All evaluated side effects have a probability of less than 50%, reflecting the low toxic risk by metabolic activation.

As the primary mediators of redox drug reactions, cytochrome P450 (CYP450) isoenzymes are responsible for forming metabolites and the plasma concentration of substances after first-pass metabolismo (Eitrich et al. 2007). Thus, it was possible to correlate the SwissADME server dataset with the in vitro parameters of the PreADMET server for inhibitors and noninhibitors of CYP 2C19, 2C9, 2D6 and 3A4, while the SOMP Online platform identified the possible Chalcone substrate sites for these due enzymes (Rudik et al. 2015). Then, the biological activity spectrum prediction method (PASS) identified the possible toxic hazards of the main Chalcone species and the possible metabolites formed by first-pass metabolism (Filimonov et al. 2014).

Pharmacophores were screened using a high-throughput screening mechanism (HTS) of the NMR ALARM rule, which identified carbonyl-associated structural alerts (C=O) adjacent to delocalized unsaturations, forming a strong nucleophilic region capable of covalently binding with proteins. Furthermore, the detected fragments of phenol and thiophene present significant biological activity in the Chalcona project since phenolic groups are potential antioxidant agents, and the thiophene ring constitutes a potential antimicrobial agent (Figure S5, supplementary material) (Stevens et al. 2003; Mishra et al. 2018). HTS is based on a series of extensive collections of compounds that constitute filters that identify possible molecular fragments with a specific biological activity. The screening technique of a La assay to detect reactive molecules by nuclear magnetic resonance (ALARM NMR) constitutes a library of reactive molecular fragments based on compounds characterized by Dithiothreitol-dependent ^{13}C NMR (DTT) as a screening method for molecular fragments with activity biological (Rishton 1997; Huth et al. 2005).

Antitarget effect prediction showed that chalcone is a potential inhibitor (-log$_{10}$[value] > 5.0) of serotonin (5-HT) receptors 1B, 2A, and 2C and dopamine 1A coupled to nerve cells, as well as adrenergic receptors α1B and α2A types and androgen (AR) and estrogen (ER) hormone receptors. In addition, the test also showed that the ligand is a potential

inhibitor of the enzyme monoamine oxidase A (MAOA) and ion transporters such as SLC6A1 and SLC6A3 (Fig. S6, supplementary material). Despite being a protein precipitator, chalcone is likely to have significant anti-inflammatory (Corroborating with the in vitro and in vivo results) ($P_a > 0.5$), antimicrobial, antiparasitic (P_a 0.49) and antiprotozoal activity of the Leishmania model (P_a 5.0) of the dataset. In addition, antioxidant, antiviral (Influenza model), and antibacterial activities have activity probabilities between $0.30 < P_a < 0.45$ (Fig. S6, supplementary material). From the evaluated toxic effects, the QNA−QSAR regressions showed that Chalcone has a predicted LD_{50} value of 977.4 mg/kg, belonging to class 4 oral toxicity, which means that the substance can be toxic by ingestion and requires a control of the oral dose administered (Diaza et al. 2015).

The degree of structural complexity of new bioactive compounds has been emphasized by medicinal chemists in the recent years. These complexities are often associated with unfavorable fitting or nonfitting to biological targets (van Laarhoven et al. 2011; Emig et al. 2013). Thus, the regression of the QSAR models of the GUSAR Antitargets tool estimates K_i and IC_{50} values ($- \log_{10}[\text{value}]$) for receptors, enzymes, and transporters. In contrast, the PASS Online tool, used in the GUSAR Online server, estimates the probability of activity (P_a) and biological and antimicrobial inactivity (P_i) by tracking similarity with the in vivo animal test dataset. At the same time, the quantitative regression of the electrotopological neighborhoods of atoms (QNA) of the GUSAR Acute Rat Toxicity tool was applied to predict the lethal dose value (LD_{50}) and the toxicity class by oral administration (Filimonov et al. 2009; Lagunin et al. 2011; Zakharov et al. 2012). The calculated physicochemical properties indicate the possibility of its use as an oral medication, while the pharmacokinetic and toxicological properties suggest an active pharmacological principle of anti-inflammatory, antioxidant, and antimicrobial activity with oral dosage control.

Conclusion

In summary, the synthesis of a new chalcone derived from a natural compound was reported and evaluated for antinociceptive, anti-inflammatory, and hypoglycemic effects in a zebrafish model. The absence of toxicity and low cytotoxicity up to specific dosages show the nonclinical safety of chalcone. In addition, evidence was provided that chalcone had an analgesic effect without causing sedative effects and/or locomotor impairment mediated by the TRPA1 system, based on the molecule's strong interactions with the TRPA1 channel. Chalcone has also shown a higher affinity for the COX-1 enzyme and excellent pharmacokinetic properties in silico. Together, these efforts provide an essential pharmacological foundation that points to this chalcone as a drug candidate or in possible formulations for treating pain, inflammation and diabetes.

Declarations

References

Adelusi TI, Du L, Chowdhury A et al (2021) Signaling pathways and proteins targeted by antidiabetic chalcones. Life Sci 284:118982. https://doi.org/10.1016/j.lfs.2020.118982

Allouche AR (2011) Gabedit: a graphical user interface for computational chemistry softwares. J Comput Chem 32:174–182. https://doi.org/10.1002/jcc.21600

Arellano-Aguiar O, Solis-Angeles S, Serrano-García L L et al (2015) Long-term response to gefitinib and crizotinib in lung adenocarcinoma harboring both epidermal growth factor receptor mutation and EML4-ALK fusion gene. J Clin Oncol 26:6005–6009. https://doi.org/10.1200/JCO.2012.47.7141

Arslanian S, Pyle L, Payan M et al (2013) Effects of metformin, metformin plus rosiglitazone, and metformin plus lifestyle on insulin sensitivity and -βcell function in TODAY. Diabetes Care 36:1749–1757. https://doi.org/10.2337/dc12-2393

Asmat U, Abad K, Ismail K (2016) Diabetes mellitus and oxidative stress—a concise review. Saudi Pharm J 24:547–553. https://doi.org/10.1016/j.jsps.2015.03.013

Bandeira PN, Lemos TLG, Santos HS et al (2019) Synthesis, structural characterization, and cytotoxic evaluation of chalcone derivatives. Med Chem Res 28:2037–2049. https://doi.org/10.1007/s00044-019-02434-1

Barr GA (1998) Maturation of the biphasic behavioral and heart rate response in the formalin test. Pharmacol Biochem Behav 60:329–335. https://doi.org/10.1016/S0091-3057(97)00602-3

Batista FLA, Lima LMG, Abrante IA et al (2018b) Antinociceptive activity of ethanolic extract of Azadirachta indica A. Juss (Neem, Meliaceae) fruit through opioid, glutamatergic and acid-sensitive ion pathways in adult zebrafish (*Danio rerio*). Biomed

Pharmacother 108:408–416. https://doi.org/10.1016/j.biopha.2018.08.160

Becke AD (1992) Densityâ functional thermochemistry. I. The effect of the exchangeâ only gradient correction. J Chem Phys. https://doi.org/10.1063/1.462066

Belo MAA, Oliveira MF, Oliveira SL et al (2021) Zebrafish as a model to study inflammation: a tool for drug discovery. Biomed Pharmacother. https://doi.org/10.1016/j.biopha.2021.112310

Bickerton GR, Paolini GV, Besnard J et al (2012) Quantifying the chemical beauty of drugs. Nat Chem. https://doi.org/10.1038/nchem.1243

Biovia DS (2016) Discovery studio modeling environment, release 2017, San Diego. Dassault Systèmes

Capiotti KM, Antonioli R, Kist LW et al (2014) Persistent impaired glucose metabolism in a zebrafish hyperglycemia model. Comp Biochem Physiol Part B 171:58–65. https://doi.org/10.1016/j.cbpb.2014.03.005

Chavan HV, Ganapure SD, Mali NN, Bhale PS (2023) Synthesis, characterization and biological evaluation of N- substituted indolyl chalcones as anticancer, anti-inflammatory and antioxidant agents. Mater Today Proc 73:396–402. https://doi.org/10.1016/j.matpr.2022.09.264

Chen G, Li C, Zhang L et al (2022) Hydroxysafflor yellow A and anhydrosafflor yellow B alleviate ferroptosis and parthanatos in PC12 cells injured by OGD/R. Free Radic Biol Med 179:1–10. https://doi.org/10.1016/j.freeradbiomed.2021.12.262

Clarke CJ, Tu WC, Levers O et al (2018) Green and sustainable solvents in chemical processes. Chem Rev 118:747–800. https://doi.org/10.1021/acs.chemrev.7b00571

Costa FV, Rosa LV, Kalueff AV, Rosemberg DB (2022) Nociception-related behavioral phenotypes in adult zebrafish. The neurobiology, physiology, and psychology of pain. Academic Press, pp 387–393

Coutinho MR, Silva AW, Ferreira MKA et al (2022) Hypoglycemic effect on adult zebrafish (*Danio rerio*) of the 3β-6β-16β-trihydroxylup-20 (29)-ene triterpene isolated from Combretum leprosum leaves in vivo and in sílico approach. Fundam Clin Pharmacol. https://doi.org/10.1111/fcp.12776

Cruz NG, Sousa LP, Sousa MO et al (2013) The linkage between inflammation and Type 2 diabetes mellitus. Diabetes Res Clin Pract 99:85–92. https://doi.org/10.1016/j.diabres.2012.09.003

Cunha ATM, Verri WA, Silva JS et al (2016) A cascade of cytokines mediates mechanical inflammatory hypernociception in mice. Proc Natl Acad Sci 102:1755–1760

da Mendes FRS, da Wlisses SA, Amâncio Ferreira MK et al (2022) GABAA receptor participation in anxiolytic and anticonvulsant effects of (E)-3-(furan-2-yl)-1-(2hydroxy-3,4,6-trimethoxyphenyl)prop-2-en-1-one in adult zebrafish. Neurochem Int 155:105303. https://doi.org/10.1016/j.neuint.2022.105303

da Rocha MN, Alves DR, Marinho MM et al (2021) Virtual screening of citrus flavonoid tangeretin: a promising pharmacological tool for the treatment and prevention of Zika fever and COVID-19. J Comput Biophys Chem. https://doi.org/10.1142/s2737416521500137

Daina A, Zoete V (2016) A BOILED-egg to predict gastrointestinal absorption and brain penetration of small molecules. ChemMedChem. https://doi.org/10.1002/cmdc.201600182

De Brito TM, Amendoeira FC, De Oliveira TB et al (2021) Anti-inflammatory activity and chemical analysis of different fractions from solidago chilensis inflorescence. Oxid Med Cell Longev. https://doi.org/10.1155/2021/7612380

de Rebouças EL, da Silva AW, Rodrigues MC et al (2021) Antinociceptive, anti-inflammatory and hypoglycemic activities of the ethanolic *Turnera subulata* Sm. flower extract in adult zebrafish (*Danio rerio*). J Biomol Struct Dyn. https://doi.org/10.1080/07391102.2021.1981449

DeLano WL (2020) The PyMOL molecular graphics system, Version 2.3. Schrödinger LLC

Diaza RG, Manganelli S, Esposito A et al (2015) Comparison of in silico tools for evaluating rat oral acute toxicity. SAR QSAR Environ Res. https://doi.org/10.1080/1062936X.2014.977819

Ditchfield R, Hehre WJ, Pople JA (1971) Self-consistent molecular-orbital methods. IX. An extended Gaussian-type basis for molecular-orbital studies of organic molecules. J Chem Phys. https://doi.org/10.1063/1.1674902

Eitrich T, Kless A, Druska C et al (2007) Classification of highly unbalanced CYP450 data of drugs using cost sensitive machine learning techniques. J Chem Inf Model. https://doi.org/10.1021/ci6002619

Emig D, Ivliev A, Pustovalova O et al (2013) Drug target prediction and repositioning using an integrated network-based approach. PLoS ONE. https://doi.org/10.1371/journal.pone.0060618

Esancy K, Condon L, Feng J et al (2018) A zebrafish and mouse model for selective pruritus via direct activation of TRPA1. Elife 7:1–24. https://doi.org/10.7554/eLife.32036

Ferreira MKA, Fontenelle ROS, Magalhães FEA et al (2018) Chalcones pharmacological potential: a brief review. Rev Virtual Quim 10:1455–1473. https://doi.org/10.21577/1984-6835.20180099

Ferreira MKA, da Silva AW, Silva FCO et al (2020) Anxiolytic-like effect of chalcone N-{4'[(2E)-3-(3-nitrophenyl)-1-(phenyl)prop-2-en-1-one]} acetamide on adult zebrafish (Danio rerio): involvement of the 5-HT system. Biochem Biophys Res Commun. https://doi.org/10.1016/j.bbrc.2020.03.129

Ferreira MKA, da Silva AW, dos Santos Moura AL et al (2021) Chalcones reverse the anxiety and convulsive behavior of adult zebrafish. Epilepsy Behav 117:107881. https://doi.org/10.1016/j.yebeh.2021.107881

Fichert T, Yazdanian M, Proudfoot JR (2003) A structure-permeability study of small drug-like molecules. Bioorganic Med Chem Lett 13:719–722. https://doi.org/10.1016/S0960-894X(02)01035-1

Filimonov DA, Zakharov AV, Lagunin AA, Poroikov VV (2009) QNA-based "Star Track" QSAR approach. SAR QSAR Environ Res. https://doi.org/10.1080/10629360903438370

Filimonov DA, Lagunin AA, Gloriozova TA et al (2014) Prediction of the biological activity spectra of organic compounds using the pass online web resource. Chem Heterocycl Compd. https://doi.org/10.1007/s10593-014-1496-1

Frisch MJ, Trucks GW, Schlegel HB, Scuseria GE, Robb MA, Cheeseman JR, Scalmani G, Barone V, Petersson GA (2016) Gaussian 16, Rev. C.01. Gaussian, Inc

Gau P, Poon J, Ufret-Vincenty C et al (2013) The zebrafish ortholog of TRPV1 is required for heat-induced locomotion. Ann Intern Med 158:5249–5260. https://doi.org/10.1523/JNEUROSCI.5403-12.2013

Gleeson M, Connaughton V, Arneson LS (2007) Induction of hyperglycaemia in zebrafish (*Danio rerio*) leads to morphological changes in the retina. Acta Diabetol 44:157–163. https://doi.org/10.1007/s00592-007-0257-3

Gonzalez-Nunez V, González AJ, Barreto-Valer K, Rodríguez RE (2013) In vivo regulation of the µ opioid receptor: role of the endogenous opioid agents. Mol Med 19:7–17. https://doi.org/10.2119/molmed.2012.00318

Grosick R, Alvarado A, Romero-Sandoval E (2017) (148) Optimizing an in vitro model using THP-1 macrophages to study pain, inflammation, and wound healing in the context of diabetes. J Pain 18:S13. https://doi.org/10.1016/j.jpain.2017.02.054

Halim M, Halim A (2019) The effects of inflammation, aging and oxidative stress on the pathogenesis of diabetes mellitus (type 2 diabetes). Diabetes Metab Syndr Clin Res Rev 13:1165–1172. https://doi.org/10.1016/j.dsx.2019.01.040

Hanwell MD, Curtis DE, Lonie DC et al (2012) Avogadro: an advanced semantic chemical editor, visualization, and analysis platform. J Cheminform. https://doi.org/10.1186/1758-2946-4-17

Heidari MR, Foroumadi A, Amirabadi A et al (2009) Evaluation of anti-inflammatory and analgesic activity of a novel rigid 3, 4-dihydroxy chalcone in mice. Ann N Y Acad Sci 1171:399–406. https://doi.org/10.1111/j.1749-6632.2009.04904.x

Huang SY, Feng CW, Hung HC et al (2014) A novel zebrafish model to provide mechanistic insights into the inflammatory events in carrageenan-induced abdominal edema. PLoS ONE. https://doi.org/10.1371/journal.pone.0104414

Huang ZH, Yin LQ, Guan LP et al (2020) Screening of chalcone analogs with anti-depressant, anti-inflammatory, analgesic, and COX-2-inhibiting effects. Bioorganic Med Chem Lett 30:1–6. https://doi.org/10.1016/j.bmcl.2020.127173

Hussain SP, Harris CC (2007) Inflammation and cancer: an ancient link with novel potentials. Int J Cancer 121:2373–2380. https://doi.org/10.1002/ijc.23173

Huth JR, Mendoza R, Olejniczak ET et al (2005) ALARM NMR: A rapid and robust experimental method to detect reactive false positives in biochemical screens. J Am Chem Soc. https://doi.org/10.1021/ja0455547

Imberty A, Hardman KD, Carver JP, Perez S (1991) Molecular modelling of protein-carbohydrate interactions. Docking of monosaccharides in the binding site of concanavalin A. Glycobiology 1:631–642. https://doi.org/10.1093/glycob/1.6.631

Jaqueline A, Bezerra N, Crisl F et al (2021) Biochemical and biophysical research communications antinociceptive effect of triterpene acetyl aleuritolic acid isolated from Croton *zehntneri* in adult zebra fi sh (*Danio rerio*). Biochem Biophys Res Commun. https://doi.org/10.1016/j.bbrc.2020.11.056

Jörgens K, Hillebrands J-L, Hammes JK (2012) Zebrafish: a model for understanding diabetic complications. Exp Clin Endocrinol Diabetes 120:186–187

Kadela-tomanek M, Jastrz M, Marciniec K et al (2021) Lipophilicity, pharmacokinetic properties, and molecular docking study on SARS-CoV-2 target for betulin triazole derivatives with attached 1, 4-quinone. Pharmaceutics 13:781. https://doi.org/10.3390/pharmaceutics13060781

Kaur B, Singh P (2022) Inflammation: biochemistry, cellular targets, anti-inflammatory agents and challenges with special emphasis on cyclooxygenase-2. Bioorg Chem 121:105663. https://doi.org/10.1016/j.bioorg.2022.105663

Khan MF, Nahar N, Bin RR et al (2018) Computational investigations of physicochemical, pharmacokinetic, toxicological properties and molecular docking of betulinic acid, a constituent of *Corypha taliera* (Roxb.) with phospholipase A2 (PLA2). BMC Complement Altern Med. https://doi.org/10.1186/s12906-018-2116-x

Kumar M, Kumar V, Singh V, Thakral S (2022) Synthesis, in silico studies and biological screening of (E)-2-(3-(substitutedstyryl)-5-(substitutedphenyl)-4,5-dihydropyrazol-1-yl)benzo[d]thiazole derivatives as an anti-oxidant, anti-inflammatory and antimicrobial agents. BMC Chem 16:1–19. https://doi.org/10.1186/s13065-022-00901-2

Lagunin A, Zakharov A, Filimonov D, Poroikov V (2011) QSAR modelling of rat acute toxicity on the basis of PASS prediction. Mol Inform. https://doi.org/10.1002/minf.201000151

Lai SC, Peng WH, Huang SC et al (2009) Analgesic and anti-inflammatory activities of methanol extract from *Desmodium triflorum* DC in mice. Am J Chin Med 37:573–588. https://doi.org/10.1142/S0192415X09007065

Lakstygal AM, De AMS, Lifanov DA et al (2019) Zebrafish models of diabetes-related CNS pathogenesis. Prog Neuropsychopharmacol Biol Psychiatry 92:48–58. https://doi.org/10.1016/j.pnpbp.2018.11.016

Lee C, Yang W, Parr RG (1988) Development of the Colle-Salvetti correlation-energy formula into a functional of the electron density. Phys Rev B. https://doi.org/10.1103/PhysRevB.37.785

Lipinski CA (2004) Lead- and drug-like compounds: the rule-of-five revolution. Drug Discov Today Technol 1:337–341. https://doi.org/10.1016/j.ddtec.2004.11.007

Lipinski CA (2016) Rule of five in 2015 and beyond: target and ligand structural limitations, ligand chemistry structure and drug discovery project decisions. Adv Drug Deliv Rev 101:34–41. https://doi.org/10.1016/j.addr.2016.04.029

Liu C, Reese R, Vu S et al (2021) A non-covalent ligand reveals biased agonism of the TRPA1 ion channel. Neuron. https://doi.org/10.1016/j.neuron.2020.10.014

Lo Faro ML, Fox B, Whatmore JL et al (2014) Hydrogen sulfide and nitric oxide interactions in inflammation. Nitric Oxide Biol Chem 41:38–47. https://doi.org/10.1016/j.niox.2014.05.014

Loetchutinat C, Kothan S, Dechsupa S et al (2005) Spectrofluorometric determination of intracellular levels of reactive oxygen species in drug-sensitive and drug-resistant cancer cells using the 2′,7′-dichlorofluorescein diacetate assay. Radiat Phys Chem 72:323–331. https://doi.org/10.1016/j.radphyschem.2004.06.011

Magalhães FEA, De Sousa CÁPB, Santos SAAR et al (2017) Adult zebrafish (*Danio rerio*): an alternative behavioral model of formalin-induced nociception. Zebrafish 14:422–429. https://doi.org/10.1089/zeb.2017.1436

Marinho EM, de Andrade B, Neto J, Silva J et al (2020) Virtual screening based on molecular docking of possible inhibitors of Covid-19 main protease. Microb Pathog. https://doi.org/10.1016/j.micpath.2020.104365

McNamara CR, Mandel-Brehm J, Bautista DM et al (2007) TRPA1 mediates formalin-induced pain. Proc Natl Acad Sci USA 104:13525–13530. https://doi.org/10.1073/pnas.0705924104

Mishra R, Sachan N, Kumar N et al (2018) Thiophene scaffold as prospective antimicrobial agent: a review. J Heterocycl Chem 55:2019–2034

Morris GM, Huey R, Lindstrom W, Lindstrom W, Sanner MF et al (2009) AutoDock4 and AutoDockTools4: automated docking with selective receptor flexibility. J Comput Chem. https://doi.org/10.1002/jcc.21256

Mosmann T (1983a) Rapid colorimetric assay for cellular growth and survival: application to proliferation and cytotoxicity assays. J Immunol Methods 65:55–63. https://doi.org/10.1016/0022-1759(83)90303-4

Mosmann T (1983b) Rapid colorimetric assay for cellular growth and survival: application to proliferation and cytotoxicity assays. RSC Adv 6:76600–76613. https://doi.org/10.1039/c6ra17788c

Nagy G, Clark JM, Buzas E et al (2008) Nitric oxide production of T lymphocytes is increased in rheumatoid arthritis. Immunol Lett 118:55–58. https://doi.org/10.1016/j.imlet.2008.02.009

Nguyen DD, Xiao T, Wang M, Wei GW (2017) Rigidity strengthening: a mechanism for protein-ligand binding. J Chem Inf Model. https://doi.org/10.1021/acs.jcim.7b00226

Orlando BJ, Malkowski MG (2016) Crystal structure of rofecoxib bound to human cyclooxygenase-2. Acta Crystallogr Sect Struct Biol Commun. https://doi.org/10.1107/S2053230X16014230

Ou Z, Zhao J, Zhu L et al (2019) Anti-inflammatory effect and potential mechanism of betulinic acid on λ-carrageenan-induced paw edema in mice. Biomed Pharmacother 118:109347. https://doi.org/10.1016/j.biopha.2019.109347

Peitsaro N, Anichtchik OV, Panula P (2000) Identification of a histamine H3-like receptor in the zebrafish (*Danio rerio*) brain. J Neurochem 75:718–724. https://doi.org/10.1046/j.1471-4159.2000.0750718.x

Qadir T, Amin A, Sharma PK et al (2022) A review on medicinally important heterocyclic compounds. Open Med Chem J. https://doi.org/10.2174/18741045-v16-e2202280

Rammohan A, Bhaskar BV, Venkateswarlu N et al (2020) Design, synthesis, docking and biological evaluation of chalcones as promising antidiabetic agents. Bioorg Chem 95:103527. https://doi.org/10.1016/j.bioorg.2019.103527

Ranjan S, Sharma PK (2020) Study of learning and memory in type 2 diabetic model of zebrafish (*Danio rerio*). Endocr Metab Sci 1:100058. https://doi.org/10.1016/j.endmts.2020.100058

Ren L, Qin X, Cao X et al (2011) Structural insight into substrate specificity of human intestinal maltase-glucoamylase. Prot Cell. https://doi.org/10.1007/s13238-011-1105-3

Reuter S, Gupta SC, Chaturvedi MM, Aggarwal BB (2010) Oxidative stress, inflammation, and cancer: how are they linked? Free Radic Biol Med 49:1603–1616. https://doi.org/10.1016/j.freeradbiomed.2010.09.006

Rishton GM (1997) Reactive compounds and in vitro false positives in HTS. Drug Discov Today 2:382–384

Rocha S, Ribeiro D, Fernandes E, Freitas M (2020) A systematic review on anti-diabetic properties of chalcones. Curr Med Chem 27:2257–2321. https://doi.org/10.2174/0929867325666181001112226

Rohm TV, Meier DT, Olefsky JM, Donath MY (2022) Inflammation in obesity, diabetes, and related disorders. Immunity 55:31–55. https://doi.org/10.1016/j.immuni.2021.12.013

Rout D, Dash UC, Kanhar S, Sandeep Kumar Swain AKS (2021) Homalium zeylanicum attenuates streptozotocin-induced hyperglycemia and cellular stress in experimental rats via attenuation of oxidative stress imparts inflammation. J Ethnopharmacol. https://doi.org/10.1016/j.jep.2021.114649

Rudik A, Dmitriev A, Lagunin A et al (2015) SOMP: web server for in silico prediction of sites of metabolism for drug-like compounds. Bioinformatics. https://doi.org/10.1093/bioinformatics/btv087

Salah T, Belaidi S, Melkemi N, Tchouar N (2016) Molecular geometry, electronic properties, MPO methods and structure activity/property relationship studies of 1,3,4-thiadiazole derivatives by theoretical calculations. Rev Theor Sci. https://doi.org/10.1166/rits.2015.1040

Shityakov S, Förster C (2014) In silico predictive model to determine vector-mediated transport properties for the blood-brain barrier choline transporter. Adv Appl Bioinform Chem. https://doi.org/10.2147/AABC.S63749

Sidhu RS, Lee JY, Yuan C, Smith WL (2010) Comparison of cyclooxygenase-1 crystal structures: cross-talk between monomers comprising cyclooxygenase-1 homodimers. Biochemistry. https://doi.org/10.1021/bi1003298

Silva FCO, de Menezes JESA, Ferreira MKA et al (2020) Antinociceptive activity of 3β-6β-16β-trihydroxylup-20 (29)-ene triterpene isolated from Combretum leprosum leaves in adult zebrafish (*Danio rerio*). Biochem Biophys Res Commun 533:362–367. https://doi.org/10.1016/j.bbrc.2020.07.107

Silverman RB, Holladay MW (2014) Lead discovery and lead modification. The organic chemistry of drug design and drug action. Elsevier, Cham

Sneddon LU (2002) Anatomical and electrophysiological analysis of the trigeminal nerve in a teleost fish, *Oncorhynchus mykiss*. Neurosci Lett 319:167–171. https://doi.org/10.1016/S0304-3940(01)02584-8

Stevens JF, Miranda CL, Frei B, Buhler DR (2003) Inhibition of peroxynitrite-mediated LDL oxidation by prenylated flavonoids: the α, β-unsaturated keto functionality of 2′-hydroxychalcones as a novel antioxidant pharmacophore. Chem Res Toxicol. https://doi.org/10.1021/tx020100d

Tang YL, Zheng X, Qi Y et al (2020) Synthesis and anti-inflammatory evaluation of new chalcone derivatives bearing bispiperazine linker as IL-1β inhibitors. Bioorg Chem 98:103748. https://doi.org/10.1016/j.bioorg.2020.103748

Trott O, Olson A (2010a) NIH public access. J Comput Chem 31:455–461. https://doi.org/10.1002/jcc.21334.AutoDock

Trott O, Olson AJ (2010b) AutoDock Vina: improving the speed and accuracy of docking with a new scoring function, efficient optimization, and multithreading. J Comput Chem 31:455–461. https://doi.org/10.1002/jcc.21334

van Laarhoven T, Nabuurs SB, Marchiori E (2011) Gaussian interaction profile kernels for predicting drug-target interaction. Bioinformatics. https://doi.org/10.1093/bioinformatics/btr500

Viana GSB, Bandeira MAM, Matos FJA (2003) Analgesic and anti-inflammatory effects of chalcones isolated from Myracrodruon urundeuva Allemão. Phytomedicine 10:189–195

Wager TT, Chandrasekaran RY, Hou X et al (2010) Defining desirable central nervous system drug space through the alignment of molecular properties, in vitro ADME, and safety attributes. ACS Chem Neurosci. https://doi.org/10.1021/cn100007x

Wager TT, Hou X, Verhoest PR, Villalobos A (2016) Central nervous system multiparameter optimization desirability: application in drug discovery. ACS Chem Neurosci 7:767–775. https://doi.org/10.1021/acschemneuro.6b00029

Wiatrak B, Kubis-Kubiak A, Piwowar A, Barg E (2020) PC12 cell line: cell types, coating of culture vessels, differentiation and other culture conditions. Cells. https://doi.org/10.3390/cells9040958

Winter CA, Risley EA, Nuss GW (1962) Carrageenin-induced edema in hind paw. Exp Biol Med 3:544–547

Xiong G, Wu Z, Yi J et al (2021) ADMETlab 2.0: an integrated online platform for accurate and comprehensive predictions of ADMET properties. Nucl Acids Res. https://doi.org/10.1093/nar/gkab255

Yan J, Zhang G, Pan J, Wang Y (2014) α-Glucosidase inhibition by luteolin: Kinetics, interaction and molecular docking. Int J Biol Macromol. https://doi.org/10.1016/j.ijbiomac.2013.12.007

Yang HH, Zhang C, Lai SH et al (2017) Isoliquiritigenin induces cytotoxicity in PC-12 Cells In Vitro. Appl Biochem Biotechnol 183:1173–1190. https://doi.org/10.1007/s12010-017-2491-7

Yee S (1997) In vitro permeability across Caco-2 cells (colonic) can predict in vivo (small intestinal) absorption in man. Fact or myth. Pharm Res 14:763–766. https://doi.org/10.1023/A:1012102522787

Yusuf D, Davis AM, Kleywegt GJ, Schmitt S (2008) An alternative method for the evaluation of docking performance: RSR vs RMSD. J Chem Inf Model. https://doi.org/10.1021/ci800084x

Zakharov AV, Lagunin AA, Filimonov DA, Poroikov VV (2012) Quantitative prediction of antitarget interaction profiles for chemical compounds. Chem Res Toxicol. https://doi.org/10.1021/tx300247r